Monitoring of freezing dynamics in trees: a simple phase shift causes complexity

Guillaume Charrier, Markus Nolf, Georg Leitinger, Katline Charra-Vaskou, Adriano Losso, Ulrike Tappeiner, Thierry Ameglio, Stefan Mayr

Plant Physiology Preview. Published on February 27, 2017, as DOI:10.1104/pp.16.01815

Short title: Monitoring of freezing dynamics in trees

Correspondence to: Dr. Guillaume Charrier

e-mail: guillaume.charrier@inra.fr

Phone: +33 5 40 00 36 64

Address: UMR 1202 Biodiversité Gènes & Communautés INRA/Université Bordeaux, Bâtiment B2 - allée G. St Hilaire, CS 50023, 33615 Pessac Cedex – France

Monitoring of freezing dynamics in trees: a simple phase shift causes complexity.

Authors

Charrier Guillaume[1,2,3]*, Nolf Markus[1,4]*, Leitinger Georg[1], Charra-Vaskou Katline[5], Losso Adriano[1], Tappeiner Ulrike[1,6], Améglio Thierry[5], Mayr Stefan[1]

[1] Department of Botany and Department of Ecology, University of Innsbruck, Sternwartestr. 15, A-6020 Innsbruck, Austria.

[2] Bordeaux Science Agro, Institut des Sciences de la Vigne et du Vin, Ecophysiologie et Génomique Fonctionnelle de la Vigne, UMR 1287, F– 33140 Villenave d'Ornon, France

[3] BIOGECO, INRA, Univ. Bordeaux, 33610 Cestas, France

[4] Hawkesbury Institute for the Environment, University of Western Sydney, Richmond, NSW 2753, Australia

[5] Université Clermont Auvergne, INRA, PIAF, F-6300 Clermont-Ferrand, France

[6] Institute for Alpine Environment, European Academy Bozen (EURAC), Drususallee 1, 39100 Bozen/Bolzano, Italy.

* Both authors contributed equally to this work

Authors' contributions: G.C., S.M., G.L. and M.N, and conceived the research plans; G.C., S.M. and M.N and performed the data monitoring (thermocouples, ultrasonic emissions and dendrometers); G.L. performed the infrared imaging; A.L. conducted additional laboratory experiments; G.C., M.N, G.L. and S.M. analyzed the data and wrote the article with contributions of all the authors.

One-sentence summary

Monitoring of freezing in timberline trees via non-destructive methods revealed complex spatial and temporal freezing patterns which promote internal water shifts and cavitation events.

Funding information

This work was supported by the Agence Nationale de la Recherche and FWF Fonds zur Förderung der Wissenschaftlichen Forschung (I826–B25 “Acoufreeze”, TA, GC, KCV, SM). MN is a recipient of a DOC-fellowship of the Austrian Academy of Sciences. We thank InfraTec for support and providing IRBIS® plus software license to conduct the requested analyses of IR images and the videos given as supplementary material.

Present address: UMR 1202 Biodiversité Gènes & Communautés INRA/Université Bordeaux, Bâtiment B2 - allée G. St Hilaire, CS 50023, 33615 Pessac Cedex – France

Phone: +33 5 40 00 36 64

e-mail: guillaume.charrier@inra.fr

Running title: Monitoring of freezing dynamics in trees

Abstract

During winter, trees have to cope with harsh conditions, including extreme freeze-thaw stress. The present study focused on ice nucleation and propagation, related water shifts and xylem cavitation as well as cell damage, and was based on *in situ* monitoring of xylem (thermocouples) and surface temperatures (infrared imaging), ultrasonic emissions and dendrometer analysis. Field experiments during late winter on *Picea abies* growing at the alpine timberline revealed three distinct freezing patterns: (i) from the top of the tree towards the base, (ii) from thin branches towards the main stem's top and base, and (iii) from the base towards the top. Infrared imaging showed freezing within branches from their base towards distal parts. Such complex freezing causes dynamic and heterogeneous patterns in water potential and probably in cavitation. This study highlights the interaction between environmental conditions upon freezing and thawing and demonstrates the enormous complexity of freezing processes in trees. Diameter shrinkage, which indicated water fluxes within the stem, and acoustic emission analysis, which indicated cavitation events near the ice front upon freezing, were both related to minimum temperature, and upon thawing, related to vapor pressure deficit and soil temperature. These complex patterns, emphasizing the common mechanisms between frost and drought stress, shed new lights on understanding winter tree physiology.

Keywords:

cavitation, dendrometer, freezing stress, ice propagation, infrared imaging, non-destructive monitoring, ultrasonic acoustic emissions, xylem embolism.

Introduction

Plants in temperate biomes can contain water under its three physical states. Liquid water flows within the xylem according to the cohesion-tension theory (Dixon, 1896), and turns into vapor in leaves. During frost days, liquid water, at least partially, changes to ice. Alpine plants are an impressive example of plants coping with these phase shifts on a frequent basis, especially in late winter to early spring, when freeze-thaw cycles can occur daily (Mayr *et al.* 2006a).

Ice formation within plants influences their physiology mechanically, hydraulically and at a cellular level (Cinotti, 1991; Charrier *et al.*, 2013a; 2015a). Mechanical strain occurs as water expands during freezing (Kubler, 1983; Cinotti, 1991) and tension is induced in the remaining liquid-phase sap (Hansen & Beck, 1988; Charrier *et al.*, 2014a; Charra-Vaskou *et al.*, 2016). Xylem cavitation is initiated on freezing due to the low (*i.e.* negative) water potential of ice (Charrier *et al.*, 2014a; Charra-Vaskou *et al.*, 2016) and the low solubility of gases in ice (Robson *et al.*, 1988; Sperry & Robson, 2001; Sevanto *et al.*, 2012). Embolism subsequently develops on thawing when gas bubbles released from the ice may coalesce, expand, and embolize the complete conduit (Sperry & Sullivan, 1992; Lemoine *et al.*, 1999; Pittermann & Sperry, 2003; Ball *et al.*, 2006; Mayr *et al.*, 2007; Mayr & Sperry, 2010; Sevanto *et al.*, 2012; Charrier *et al.*, 2014a; Charra-Vaskou *et al.*, 2016). The low water potential of ice also generates an osmotic disturbance on macro-molecule arrangement, which can lead to membrane breakage and cellular lysis (Pearce, 2001; Uemura *et al.*, 2006; Ruelland *et al.*, 2009).

When temperatures drop below 0°C, the xylem sap remains in a metastable, supercooled state (Wolfe & Bryant, 2001) until crystallization is initiated around a *nucleus*. Ice nucleation can occur when water molecules form long enough transitory hydrogen bonds with each other,

94 reaching a critical nucleus size of 1.13 nm, containing *ca*. 190 molecules (*i.e.* homogeneous
95 nucleation at temperatures below -38°C), or onto a nucleating agent (heterogeneous
96 nucleation onto impurity, cell wall, or Ice Nucleation Active bacteria; Sakai & Larcher, 1987).
97 In trees, ice nucleation is generally observed in the apoplastic compartment (Asahina, 1956),
98 through intrinsic heterogeneous nucleation (Wisniewski *et al.*, 1997; Pearce, 2001). Once
99 started, ice propagates through the plant, radially and longitudinally (Neuner *et al.*, 2010).

100 The physical transition from a disordered liquid state to an ordered crystal structure is an
101 exothermic reaction, which releases latent heat (334 $J \cdot g^{-1}$; Dereudre & Gazeau, 1992) and
102 entraps gas bubbles emerging from solution (Sperry & Robson, 2001; Sevanto *et al.*, 2012). A
103 freezing exotherm can therefore be detected using thermocouples (*e.g.* Mayr *et al.*, 2006a;
104 Pramsohler *et al.*, 2012) or infrared imaging (Wisniewski *et al.*, 1997; Hacker & Neuner,
105 2007; Charrier *et al.*, 2015a). Exotherm monitoring is widely used to detect freezing in plants,
106 but this technique is very limited at detecting much slower phenomena such as thawing. At
107 thawing, xylem sap becomes liquid through an opposite endothermic reaction.

108 Further insights into freezing and thawing processes were enabled by dendrometers (Zweifel
109 & Häsler, 2000) and ultrasonic emission analysis (Charrier *et al.*, 2015a). Dendrometers are
110 commonly used to monitor growth and drought stress in woody plants (Reineke, 1932;
111 Daubenmire, 1945; Deslauriers *et al.*, 2007; de Swaef *et al.*, 2015). However, upon freezing, a
112 sharp decrease in diameter is observed in the bark of acclimated plants, which is probably
113 caused by water fluxes towards the ice nucleation point in intercellular spaces (Zweifel &
114 Häsler, 2000; Ball *et al.*, 2006; Charra-Vaskou *et al.*, 2016). On thawing, the initial diameter
115 is restored, but only partly in plants that are not fully acclimated (Améglio *et al.*, 2001). The
116 proportion of irreversible diameter shrinkage can therefore serve as an assessment of frost-
117 induced damages to living cells (Lintunen *et al.*, 2015). Ultrasonic emission (UE; Mayr *et al.*,
118 2007) analysis is a non-destructive technique which detects spontaneous liquid to vapor phase

transitions (*i.e.* cavitation events) under drought (Milburn, 1966; Tyree & Dixon, 1983; Mayr & Rosner, 2011; Vergeynst *et al.*, 2014; Nolf *et al.*, 2015) or frost stress (Kikuta & Richter 2003; Mayr *et al.*, 2007; Charrier *et al.*, 2014a). The latter is likely based on bubble formation due to the low water potential of the xylem sap near growing ice fronts. When the water potential reaches the cavitation threshold, gas bubbles form, and the sudden relaxation of water columns generates UEs. Recently, the UE technique was used to monitor ice propagation within branches in laboratory experiments (Charrier *et al.*, 2015a), and UE velocity and attenuation were shown to enable the detection of ice in woody stems (Charrier *et al.* 2014b). UE were also observed during thawing, in relation with embolism formation according to the thaw-expansion hypothesis (Mayr & Sperry, 2010).

In trees, the dynamics of freezing and resulting occurrence of ice in the axis system have a crucial effect for hydraulics (*e.g.* increased levels of frost-induced embolism in distal parts of branches; Lemoine *et al.*, 1999). Frozen xylem in the trunk blocks water uptake from the soil and thus supply to distal parts such as the leaves of evergreens. Ice in branches disconnects the hydraulic continuum within the plant and thus prevents equilibration of water potentials, which may cause complex within-plant variation in drought stress intensities (Mayr & Charra-Vaskou, 2007), especially when high evaporative demand and frozen soil are concomitant (Mayr *et al.*, 2002; 2006b; 2014). This complexity is further increased by the spatio-temporal pattern of ice and respective frost damages in dead (xylem embolism) and living tissues (cell damage).

Ice nucleation usually occurs where the local (organ) temperature reaches the freezing point. Under field conditions, air temperature is often considered as a proxy for organ temperature. However, temperature varies spatially, being lower close to the ground in an open environment (Leuning & Cremer, 1988; Jordan & Smith, 1994; Battany, 2012) or, in more closed stands, at the air-plant interface (Tappeiner 1985; Winkel *et al.*, 2009). Compared to

144 air temperature, plant organ temperature exhibits a buffered response due to thermal inertia of
145 the local wood section (proportional to stem diameter) and isolating layers (*e.g.* bark). The
146 actual temperature in plant tissues therefore is the result of the energy balance driven by net
147 radiation, air temperature, humidity and soil calorific capacity (Cellier, 1984; 1993; Leuning,
148 1988; Jordan & Smith, 1994). Thus, freezing and thawing patterns are complicated by
149 temperature variation, *e.g.* due to microclimatic factors, topography and crown architecture,
150 or the latent heat released by ice formation. Additionally, tissues with more negative osmotic
151 potentials exhibit lower freezing points (Sakai & Larcher, 1987; Yelenosky & Guy, 1989),
152 which in turn influences the spatial pattern of potential ice nucleation.

153 We hypothesized that late winter environmental conditions result in disturbances in the plant
154 hydraulic system, which generate ice formation and propagation from the coldest organs of
155 the tree (*e.g.* the apex, or thin side branches) towards the base. To test this hypothesis, we
156 monitored ice formation and propagation within the trunk and crown of *Picea abies* trees
157 growing near the alpine timberline using non-destructive methods (thermocouples, infrared
158 imaging, and UE analysis; Fig. 1). It is known that timberline trees are exposed to numerous
159 and intense freeze-thaw cycles (see above) and thus provide an ideal system to study
160 respective dynamics. Furthermore, an analysis of these patterns is essential to understand the
161 impact of winter conditions on tree physiology at higher elevation. Xylem (*via*
162 thermocouples) and surface temperature (*via* infrared imaging) were used to detect freezing
163 occurrence and ice propagation. UE analysis should enable to detect xylem sap cavitation,
164 either upon freezing or thawing, and dendrometry to detect water shifts and cellular damage,
165 in relation with environmental conditions.

166 ## Results

During four successive late winter periods, we recorded 15 independent freezing processes within the tree crown via exotherm detection in the xylem (thermocouples). Three different patterns of freezing exotherms within the crown, with respect to temporal and spatial courses, were observed: (i) from the top downwards to the basal part of the tree (approx. 20% of observations, Fig. 2A-B, March 19, 2013), (ii) from the base upwards to the tree top (approx. 30% of observations, Fig. 2C-D, March 22, 2013), (iii) from side branches to the stem and up- and downwards (approx. 50% of observations, Fig. 2E-F, March 13, 2015). Ice propagated at approx. 1 to 4 $mm \cdot s^{-1}$ in up- and downward directions.

Infrared image analysis allowed us to map changes in surface temperature across a large part of the tree, highlighting a more complex freezing pattern than indicated by exotherm analysis based on single, individually placed thermocouples. For instance on March 14, 2015 (Fig. 3; supplementary video 1), before freezing occurred (17:00), a vertical gradient in surface temperature was observed along the trunk from the middle (T_3, approx. -2°C) to the apex (T_1, approx. -2.5°C), and side branches (B approx. -3°C). From 17:46 to 18:15, exotherms indicated that freezing started from the branch base and moved towards the distal parts of branches, respectively. However, the pattern within the crown appeared as spatially erratic, with seemingly independent exotherms detected in different side branches. Overall, branches inserted at middle height froze before higher and lower branches. Although the increase in trunk surface temperature was too low to be visually detected on the video, temperature dynamics extracted from infrared image analysis (Fig. S1A, B) were in agreement with the dynamics observed via thermocouples (Fig. S1C, D). On side branches, exotherms were recorded earlier with thermocouples than with infrared imaging, because the latter recorded temperature changes at the surface while thermocouples were installed directly in the xylem. In the apical and middle parts of the trunk (T_1-T_3), exotherms were concurrently detected with thermocouple and infrared imaging, indicating a stronger exotherm signal based on a much

192 larger volume of freezing wood. The freezing patterns of a second tree (tree 2, at the right in
193 the supplementary video), and during other freezing events (March 25-27, 2014 or March 13-
194 14, 2015) were similar, with side branches at middle height freezing before branches near the
195 apex or the base.

196 Upon freezing, UEs were detected concurrently with exotherm formation within the trunk as
197 measured by thermocouples (March 7, 2012; Fig. 4): from the lower (T_5, UE: 17:48; TC:
198 17:53) to the upper position (T_2, UE: 18:00; TC: 17:57). While the onset of UEs thus clearly
199 corresponded to freezing, consecutive acoustic activity did not exhibit a clear spatial pattern,
200 and UEs were detected long after the exotherm had dissipated (Fig. 5). Ultrasonic emissions
201 exhibited two phases of activity within a daily freeze-thaw cycle *i.e.* a phase from the onset of
202 freezing (indicated by a freezing exotherm) until sunrise, and a second phase after the xylem
203 had thawed in the morning until sunset (March 12-13, 2015, Fig. 5). Of the high number of
204 UEs recorded during the different monitoring periods (approx. 760,000 UE), 52% were
205 recorded in the side branch (B), 29% in the middle of the trunk (T_3), 15% in the upper portion
206 of the trunk (T2), and only 3.5% in the lower part (T5), with similar trends for day and
207 nighttime activities.

208 The two phases of acoustic activity were remarkably associated with decreasing trunk
209 diameter, however, to a different extent (March 12-13, 2015, Fig. 5). Daytime UE activity
210 (approx. 0.07 UEs·s^{-1}) and decreasing trunk diameter (-100µm; -0.01µm·s^{-1}) were observed as
211 long as temperature remained above 0°C (16:00). After sunset, the second phase of UE
212 activity (0.45 UEs·s^{-1}) started once the freezing exotherm reached a plateau (19:30),
213 concurrent with diameter shrinkage (-175µm; -0.12µm·s^{-1}). Finally, another peak in UE
214 activity (2.25 UEs·s^{-1}), was recorded when the xylem differential temperature (xylem
215 temperature - air temperature; $dT_{xylem-air}$ = +2.7°C at 0:00) started to decrease, again
216 associated with trunk diameter shrinkage (-400 µm; -0.12µm·s^{-1}; Fig. 5). During the

intermediate periods of low UE activity (*e.g.* plants thawing from 08:20 until 10:20, or at the onset of freezing from 17:00 until 19:30) the stem recovered its initial diameter.

During March 12-17, 2015, we observed a period of pronounced daily temperature fluctuations. Temperatures exhibited high diurnal amplitudes of 10-15K as well as increasing minimum and maximum temperatures and corresponding vapor pressure deficits (Fig. 6A). Since March 14, minimum temperature progressively increased, resulting in lower UE activity and higher minimum diameter at night (Fig. 6B). However, UE activity during daytime increased over this period, in relation with temperature (>5°C), and VPD (> 500 kPa). Interestingly, nighttime freezing generated approx. 10 times higher diameter shrinkage than daytime thawing, whereas maximum UE activity was three times lower at night than during the day (Fig. 6B). Furthermore, UEs were almost completely restricted to periods of diameter shrinkage (approx. 87% of total recorded UEs).

Nighttime UE activity and diameter shrinkage were negatively correlated with minimum air temperature ($R^2 = 0.509$, $P < 0.001$ and $R^2 = 0.410$, $P = 0.042$ for UEs and diameter, respectively; Fig. 7A; Tab. I). During the day, UE activity and diameter shrinkage were correlated with minimum soil temperature ($R^2 = 0.303$, $P < 0.001$ and $R^2 = 0.559$, $P = 0.008$ for UEs and diameter, respectively; Fig. 7B). However, day- and nighttime UE activities were related to temperatures via exponential functions, whereas diameter shrinkages via linear functions. UE activity was, consequently, exponentially correlated to diameter shrinkage ($R^2 = 0.233$, $P = 0.031$; Fig. 7C), with no significant difference between day and night ($P = 0.124$). Correlations between maximum VPD and UEs ($P = 0.049$), and between diameter shrinkage and minimum air temperature were also observed ($P = 0.002$). Furthermore, the maximum VPD observed during the same night was correlated with both nighttime UEs ($P = 0.015$) and diameter shrinkage ($P < 0.001$).

Discussion

This study shows that freezing plant tissues do not just undergo a simple phase shift. Instead, UEs and stem diameter variation revealed that ice nucleation is only the onset of a complex series of internal changes that continue several hours beyond the initial exotherm formation (Fig. 5, Fig. 8). These changes may promote sap cavitation upon freezing and thawing in environmental conditions typical for early spring (*i.e.* low air and soil temperature, high VPD). Remarkably, even once most of the sap was in solid state, the frozen branch underwent changes as indicated by subsequent radial stem (*i.e.* bark) shrinkage and increasing UE activity with decreasing air temperatures (Fig. 6, Fig. 7, Tab. 1). Both of these effects were correlated with soil temperature and VPD and likely resulted from the low water potential of ice, which depends on the degree of supercooling (-1.16 $MPa \cdot K^{-1}$; Hansen & Beck, 1988). Upon freezing, radial water fluxes and related cavitation events increased the heterogeneity in water distribution within the tree crown. Such conditions are expected to favor embolism development on thawing, when the root system cannot compensate for evaporative water losses (Fig. 8).

The remarkable correlation between diameter shrinkage and UE activity (Fig. 5-7) indeed indicates that water fluxes are generated towards the ice nucleation point (Cavender-Bares, 2005; Ball *et al.*, 2006). These water fluxes resulted in bark shrinkage and increased the tension in the remaining liquid xylem sap (Charra-Vaskou *et al.*, 2016). When the cavitation threshold was reached, UE were generated (Charrier *et al.*, 2014b), in relation with freezing velocity (Charrier *et al.*, 2015a). Furthermore, cavitation-related UEs may be generated when air is expelled from the crystal lattice during freezing and gets pulled through pits (Mayr *et al.*, 2007; Charrier *et al.*, 2014b; Charrier *et al.*, 2015a). Such air bubbles can then expand at thawing and, especially while the xylem sap is under tension (Mayr & Sperry, 2010), fill and therefore embolize the whole conduit (Ball *et al.*, 2006; Charra-Vaskou *et al.*, 2016).

While ice nucleation and its related effects typically occur at night, UE activity and decreasing stem diameter were also observed during the day period (Fig. 5, Fig. 6, Tab. 1). Daytime UE activity increased with vapor pressure deficit (VPD) and decreasing soil temperature. The observed diameter shrinkage indicates that the water supply could not compensate the evaporative demand, resulting in increasing drought stress during sunny days ('winter drought'; Sakai & Larcher, 1987; Tranquillini, 1979), as previously described for mountainous areas (Michaelis, 1934a; 1934b; Henson, 1952; Larcher, 1957; 1977; Wardle, 1971; Tranquillini, 1979). Cavitation events thus occurred not only on freezing but also on thawing, which over the course of many freeze-thaw cycles can lead to high levels of winter embolism (*e.g.* Mayr *et al.*, 2003; 2006b). Day- and nighttime environmental conditions therefore interact in water redistribution within the tree crown, which exponentially increases the probability of cavitation events (Fig. 7). Embolism repair and hydraulic recovery, which do not produce UEs, may mitigate this hydraulic limitation, and have indeed been observed in *Picea abies* even while the soil was frozen (Mayr *et al.*, 2006b; 2014). Furthermore, insulation from VPD due to snow cover helps small trees and shrub species to avoid or reduce drought stress during winter months (Larcher, 1963).

Freeze-thaw cycles in winter and early spring are common in temperate to boreal and mountainous regions. The study site at the timberline and the late-winter season were chosen as the ideal place and time to observe them *in situ*, with broad daily thermal amplitudes due to topography, high elevation (1600 m a.s.l.), south-east exposure, and an open stand (Blennow, 1998; Blennow & Persson, 1998). Such conditions are particularly favorable for radiative freezing events to occur in late winter (Monteith & Unsworth, 1990; Lindkvist *et al.*, 2000; Charrier *et al.*, 2015b). During this period, when the sky is clear, the energy balance is usually positive at daytime (solar radiation > 600 $W \cdot m^{-2}$) and negative at night (long-wave infrared radiation dissipated to clear sky; Nobel, 1987; Snyder & Melo-Abreu, 2005). Air temperature

291 during the study period thus alternated on average from -4.4°C (nighttime) to +7°C (daytime),
292 but extreme daily thermal amplitudes can reach up to 30 K in alpine conditions (Mayr *et al.*,
293 2006a). Local sunset at the study site was between 16:00 and 17:00 (surrounding mountains
294 approx. 20° above horizon), resulting in a negative net energy income of the ecosystem. A
295 rapid decrease in air temperature (6.3 $K \cdot h^{-1}$ on average) therefore led to fast freezing events.
296 In the morning, the temperature increased at an even faster rate (8.1 $K \cdot h^{-1}$ on average) and
297 thus temperature changes were overall faster than generally reported (approx. 5 $K \cdot h^{-1}$; Levitt,
298 1980; Sakai & Larcher, 1987). During the monitored period, the fastest rates of temperature
299 change were similar for cooling (-14.5 $K \cdot h^{-1}$; Apr 7, 2015) and warming (+15.8 $K \cdot h^{-1}$; March
300 7, 2012). Cooling, however, was far slower than rates at which intracellular freezing and thus
301 cellular damage was reported (-48 $K \cdot h^{-1}$; Levitt, 1958; Siminovitch *et al.*, 1978). Accordingly,
302 stem diameters fully recovered to initial values after thawing (Fig. 5, Fig. 6), indicating that
303 living tissues were still intact (Améglio *et al.*, 2001; Lintunen *et al.*, 2015; Charra-Vaskou *et*
304 *al.*, 2016). Also minimum temperatures were not critical, as plants can usually suffer
305 temperatures as low as -40°C without significant cell damage (Christersson, 1978; Repo,
306 1992; Charra-Vaskou *et al.*, 2012) before de-acclimation during the spring period.

307 The delay between the onset of exotherm formation (17:00) and diameter shrinkage (20:35),
308 as well as the two phases observed in diameter shrinkage (before/after 21:50) suggest that the
309 spatiotemporal pattern of freezing was heterogeneous (Fig. 5). Although exotherms observed
310 via thermocouples revealed freezing of xylem tissue, the diameter remained unaffected for
311 one to three hours (Fig. 5, Fig. 6). As long as the stem remained warmer than air, the ice water
312 potential did not compensate the intra-cellular osmotic potential (Cavender-Bares 2005;
313 Charrier *et al.*, 2013b), nor reach the cavitation threshold (Charrier *et al.*,; 2015b). However,
314 as the exothermal heat dissipated, liquid water was pulled from the cytoplasm toward the
315 apoplasm, leading to cell plasmolyis (Uemura *et al.*, 2006; Ruelland *et al.*, 2009), diameter

316 shrinkage (Charra Vaskou *et al.*, 2016) and UEs (Kasuga *et al.*, 2014; Charrier *et al.*, 2015b) .
317 Because of their higher elasticity, bark tissues exhibit more pronounced thickness changes
318 upon freezing than xylem (Zweifel & Hasler, 2000; Améglio *et al.*, 2001). The extracellular
319 freezing of the bark tissues was probably the trigger of water fluxes outwards from the xylem,
320 and the resulting tension generated UE. Other elements than the xylem conduits have been
321 shown to generate UEs on freezing in angiosperms, such as bark (Kikuta, 2003) or xylem
322 parenchyma (Kasuga *et al.*, 2014).

323 Ice nucleation is partly a stochastic process *i.e.* freezing depends on the interaction between
324 low temperature and the presence of a *nucleus*. In our study, the lowest temperatures were
325 generally observed in the apex and branches, whereas, surprisingly, freezing sometimes also
326 started from the base of the trunk (Fig. 2 A-F, 3). We observed three distinct freezing patterns
327 in the same *Picea abies* tree (Fig. 2, 8): (i) Ice propagated from the base, when this part
328 remained frozen during the entire day while the upper crown thawed in the sun. (ii) Ice
329 nucleation occurred in the apex and the ice then spread downwards. (iii) Freezing started in
330 branches, with the ice front seemingly moving towards the main axis. These last two freezing
331 patterns would suggest that the distal parts of the tree (apex or branches) experienced lower
332 temperatures, which therefore had increased probability for nucleation. However, infrared
333 image analysis showed a more detailed picture: ice nucleation in branches occurred close to
334 the base of the branch and propagated towards the distal ends (see supplementary video).
335 These observations do not only show that the presence of metallic sensors in contact with the
336 xylem did not induce 'artificial' ice nucleation. They also suggest that a lower temperature in
337 branches (compared to the trunk), combined with larger conduits (at the branch base
338 compared to distal branch sections) may increase the probability for ice nucleation (Asahina,
339 1956; Lintunen *et al.*, 2013) and, in consequence, make the base of branches a likely ice
340 nucleation site. Additional freezing experiments in the laboratory, where the direction of ice

propagation was determined in excised branch segments, could not confirm this pattern consistently (data not shown). However, these laboratory experiments could not simulate the microclimatic effect of dense needle cover in the distal portion of the branch, which might have buffered the temperature decrease.

Once nucleated, the ice front can propagate after the exothermal heat has dissipated through the bark (Shibkov *et al.*, 2003), whereby propagation rates within the water column are proportional to the degree of supercooling (Langer *et al.*, 1978; Rauschenberger *et al.*, 2013). In excised branches from *Picea abies*, propagation rates similar to the present field study were observed (2 and 4 $mm \cdot s^{-1}$, for 1.5 and 2 K of supercooling, respectively; Charrier *et al.*, 2015a). Ice propagation towards the distal end of a branch can generate two opposite effects on sap water potential: (i) The density of ice with respect to liquid water (917 *vs* 1000 $kg \cdot m^{-3}$ at 0°C, respectively) induces an approx. 9% increase in local pressure (Hare & Sorensen, 1987; Holten *et al.*, 2012), and (ii) the tension induced by ice is approx. 1.16 $MPa \cdot K^{-1}$ (Hansen & Beck, 1988). Ice nucleation in the basal part of the branch thus can pull liquid sap from the distal end, which redistributes water toward nucleation sites (Ball *et al.*, 2006; Charra-Vaskou *et al.*, 2016), explaining the gradient in water potential and higher embolism observed under similar conditions (Mayr & Charra-Vaskou, 2007), and the higher number of UEs in branches than in any other part of the trunk. Nevertheless, during daytime, distal ends most likely thawed first and, hydraulically disconnected from the rest of the plant, would subsequently experience higher levels of drought stress and embolism compared to basal parts (Lemoine *et al.*, 1999). Such a spatial distribution of embolism within the plant may prevent embolism from spreading towards the base when the soil is frozen.

The present study reveals an enormous complexity in freezing dynamic and ice distribution within trees (Fig. 8). We showed that ice fronts may diverge into different directions within a stem or collide in other stem sections, which may cause separation of the hydraulic continuum

unless ice blockages dissolve during thawing. The combined use of several sensing technologies enabled us to demonstrate not only contrasting ice propagation patterns, but also the link between ice formation, diameter changes due to water shifts and ultrasonic activity due to cavitation. These processes are highly relevant for plant hydraulics and freezing stress, and their understanding is a prerequisite for studies on winter stress not only in timberline species but also for temperate trees in general.

Material and methods

Study site and tree description

Study trees were naturally growing in Praxmar (Tyrol, Austria; 47°09′N; 11°07′E; 1680 m a.s.l.) close to the timberline. Two Norway Spruce trees (*Picea abies* L. Karst), located on the edge of the closed forest, were monitored during late winter. One tree was completely isolated from surrounding trees (thereafter called tree 1), whereas the other one was located closer to surrounding trees (thereafter called tree 2). Tree 1 was monitored repeatedly during four successive years from 2012 until 2015, whereas tree 2 was only monitored during late winter 2015. Both trees were similar in dimension although growing during the four monitored years: height from approx. 2.5 to 4 m, diameter at breast height from 5 to 10 cm. The monitoring period ranged from early March until late April, at a period when frequent diurnal freeze-thaw cycles are known to occur. At that time, a snow cover was still present and the soil frozen. Freezing events were monitored with different sensors (thermocouples, UE sensors, and dendrometers) at six positions along the main axis, from trunk base to top, and on a side branch (Fig. 1). Depending on the availability of equipment, installations were made in different combinations.

Temperature measurements

390 Xylem and air temperature were monitored using copper-constantan thermocouples connected
391 to a datalogger (1000 Series Squirrel Meter/Logger, Eltek, Cambridge, UK) at 30-60 s
392 interval. Thermocouples were installed in the xylem at 0.5-1 cm depth at 6 positions, along
393 the main trunk (apex: T_1 to base: T_5) and on a side branch (B), and attached using Terostat
394 putty (Henkel, Düsseldorf, Germany).

395 **Infrared imaging**

396 Surface temperature was recorded using a thermal infrared camera (Jenoptik VarioCam® HR,
397 InfraTec, Jena, Germany) at approx. 7 m distance from the trees. This camera is sensitive to
398 radiation at 7.5–14 μm wavelength of the electromagnetic spectrum with a temperature
399 resolution < 0.08 K. Thermal images (thermograms) were recorded at 0.025 m focal length,
400 resulting in 384 x 288 pixel images at approx. 0.01 $m^2.pixel^{-1}$ spatial resolution. Thermograms
401 were recorded every 5 seconds, and processed using *IRBIS*® 3 *plus* software (InfraTec, Jena,
402 Germany).

403 **Ultrasonic emission analysis**

404 UEs were monitored on Tree 1 with a 4-channel USB based system (1283 USB AEnode, 18-
405 bit A/D, 20 MHz) and 150 kHz 26 dB pre-amplified resonance sensors (PK15I; all
406 components: Physical Acoustics, Wolfegg, Germany) set to 20 dB threshold. On Tree 2, an
407 autonomous AE system device was installed, also equipped with four 150 kHz 26 dB pre-
408 amplified resonance sensors (PK15I; all components: Mistras, Sucy-en Brie, France).
409 Registration and analysis of ultrasonic events were performed with AEwin software vE.4.40
410 (Mistras Holdings Corp., Princeton, USA). Acoustic sensors were attached using spring-
411 loaded clamps at three positions along the trunk (T_2, T_3, T_5) and on a side branch (B; Fig. 1)
412 after removing approx. 1 cm^2 of bark and covering the exposed xylem with silicone grease to
413 ensure the acoustic coupling and prevent dehydration. Acoustic coupling was tested with lead

414 breaks (Hsu Nielsen method; Kalyanasundaram *et al.*, 2007; Charrier *et al.*, 2014b) at a
415 distance of 1 cm from each sensor, and sensors were re-installed when the signal amplitude
416 was below 90 dB.

417 **Micro-dendrometers**

418 Diurnal and longer-term variation in stem diameter was monitored using dendrometers on
419 both trees during late winter 2015. A PépiPIAF system (Forest Future, Nancy, France) was
420 installed in the upper third of the main axis (between T_2 and T_3, Fig. 1) of each tree. Each unit
421 contains a linear variable differential transformer (LVDT) sensor (sensitivity ±1 µm)
422 connected to a data logger recording at 5 min interval.

423 **Supplemental material**

424 Figure S1. Freezing patterns monitored via infrared imaging (A, B) and thermocouples (C, D).

425 Supplementary video S1 shows the temporal progression of differential surface temperatures
426 of a *Picea abies* tree and the surrounding snow cover, recorded by infrared imaging on March
427 14, 2015.
428 Supplementary video S2 shows an example of poikilothermic vs homeothermic regulation in
429 alpine winter conditions, recorded on the evening of March 3, 2011.

430

431 **Figure captions**

432 **Figure 1.** Measurement setup and sensor positions along a *Picea abies* tree.

433 **Figure 2.** Freezing patterns as observed via freezing exotherms along a *Picea abies* tree
434 growing at the alpine timberline after sunset using thermocouples inserted into the xylem.
435 Left panels (A, C, E) show absolute temperatures during one evening. Right panels (B, D, F)

present differential thermal analysis (xylem – air temperature) during the same freezing events. Arrows indicate the onset of exotherms at different sensor positions (B, T_1-T_5) according to Fig. 1.

Figure 3. Spatial temperature patterns in a *Picea abies* tree growing at the alpine timberline at the time of freezing (after sunset; onset at approx. 17:55) monitored via infrared imaging. Letters (B, T_1-T_4) indicate sensor positions (see Fig. 1), arrows indicate additional positions with very pronounced changes. Note different time scales in the upper vs. lower row. Upper grey panels (A) show temperature changes over two hours within the crown. Lower panels (B) illustrate the period when xylem exotherms were detected (17:55 to 18:05). This timeframe thus corresponds to the onset of the freezing, and areas with pronounced events were highlighted in the thermograms.

Figure 4. Sequence of freezing exotherms observed using thermocouples (differential thermal analysis, xylem - air temperature; A) and cumulated ultrasonic emissions (UEs; B) in a *Picea abies* tree during a freezing event. Arrows indicate the onset of exotherms at different sensor positions (B, T_2, T_3, T_5).

Figure 5. Ultrasonic activity (A) and stem diameter changes (B) in a *Picea abies* tree during a freezing event. Temperatures are given as absolute (T_3, Air; A) and differential (xylem - air temperature; B) values. Stem diameter is given as differential with respect to initial diameter (*i.e.* Day 1, 12:00) to highlight dynamic changes. Vertical dashed lines indicate the onset of the exotherms as observed using thermocouple data.

Figure 6. Diurnal sequences of environmental conditions (air and xylem temperature, vapor pressure deficit; A), stem diameter changes, and ultrasonic activity (B) in a *Picea abies* tree during six days with five freeze-thaw cycles. Stem diameter is given as differential with

459 respect to initial diameter (*i.e.* Day 1, 12:00) to highlight dynamic changes. Vertical dashed
460 lines indicate the onset of the freezing exotherms as observed by thermocouples.

461 **Figure 7.** Average ultrasonic activity (filled dots) and diameter shrinkage (white dots)
462 observed per night (net radiation < 10 $W.m^{-2}$) depending on average air temperature (A), or
463 per day depending on average soil temperature (B). Average ultrasonic activities depending
464 on diameter shrinkage (C) are presented with no significant difference between day (white
465 diamonds) and night (filled diamonds). Note that y-scales are logarithmic; R^2 values apply to
466 exponential (UEs activities), or linear fits (diameter shrinkage).

467 **Figure 8.** Generalized scheme of observed patterns and underlying water fluxes in a *Picea*
468 *abies* tree during a freeze-thaw cycle in late winter. Initial equilibrated state (A), ice
469 nucleation and propagation with associated water fluxes, stem shrinkage and ultrasonic
470 emissions (B), ultrasonic activity after exotherm dissipation (C), stem diameter increase and
471 developing water potential gradient during thawing (D), and stem shrinkage and high
472 ultrasonic activity during daytime transpiration with frozen soil (E).

473

474

475

476

477 **Figure S1.** Freezing patterns monitored via infrared imaging (A, B) and thermocouples (C,
478 D).

479 **Supplementary video 2.** Dynamic change of surface temperature in *Picea abies* and *Lepus*
480 *europaeus* recorded by infrared image analysis at 1 s interval on March 3, 2011.

Supplementary video 1. Dynamic change of surface temperature in two *Picea abies* trees growing at the timberline, recorded by infrared image analysis at 5 s interval on March 14, 2015.

Figure S1. Freezing patterns monitored via infrared imaging (A, B) and thermocouples (C, D). Left panels (A, C) show absolute temperatures, right panels (B, D) show differential thermal analysis (xylem - air temperature) during the same freezing event. Arrows indicate the onset of exotherms at different sensor positions (B, T_1, T_3) according to Fig. 1.

Supplementary video 1. Dynamic change of surface temperature in two *Picea abies* trees growing at the timberline, recorded by infrared image analysis at 5 s interval on March 14, 2015. The video shows differential temperatures between 17:45 and 18:30, based on a reference frame recorded at 17:45. Warmer areas appear brighter, and areas where temperature was more than 1K above the reference temperature appear in red. Markers indicate the positions of the thermocouple sensors (T_1, T_2, T_3, T_4, B).and ultrasonic sensors (T_2, T_3, B).

Supplementary video 2. Dynamic change of surface temperature in *Picea abies* and *Lepus europaeus* recorded by infrared image analysis at 1 s interval on March 3, 2011. at approx. 19:15. This is a typical example of poikilothermic (*P. abies*) vs. homeothermic (*L. europaeus*) regulation in alpine winter conditions.

500 **Acknowledgements**

501 This work was supported by the Agence Nationale de la Recherche and FWF Fonds zur
502 Förderung der Wissenschaftlichen Forschung (I826–B25 "Acoufreeze", TA, GC, KCV, SM).
503 MN is a recipient of a DOC-fellowship of the Austrian Academy of Sciences. We thank
504 InfraTec for support and providing an IRBIS® plus software license to analyze and visualize
505 infrared imaging data.

506

507 **Table I.** Spearman's correlation coefficient ρ between stem diameter variation, cumulated ultrasonic
508 emissions observed during day and night periods and environmental variables *i.e.* minimum air
509 temperature, minimum soil temperature and maximum vapor pressure deficit. Because of the
510 particular local conditions, night-day shift was selected based on a threshold in net incoming
511 radiation equal to 10 $W \cdot m^{-2}$. Different symbols refer to *P*-value: *** *P*< 0.001; ** *P*< 0.01; * *P*<0.05; ^{ns}
512 not significant.

513

		df	Minimum air temperature	Minimum soil temperature	Maximum vapor pressure deficit
Night	Diameter change	33	-0.351*	0.325^{ns}	-0.877***
	Ultrasonic emission	38	-0.753***	-0.168^{ns}	-0.387*
Day	Diameter change	33	-0.511**	-0.451**	0.273^{ns}
	Ultrasonic emission	37	-0.219^{ns}	-0.575***	0.322*

514

515

516

517

518

519

520

521 **References**

522 Améglio T, Cochard H, Ewers F (2001) Stem diameter variations and cold hardiness in
523 walnut trees. J Exp Bot 52: 2135–2142

524 Asahina E (1956) The freezing process of plant cell. Contrib Inst Low Temp Sci Hokkaido
525 Univ 10: 83–126

526 Ball MC, Canny MJ, Huang CX, Egerton JJG, Wolfe J (2006) Freeze/thaw-induced
527 embolism depends on nadir temperature: the heterogeneous hydration hypothesis. Plant Cell
528 Environ 29: 729–745

529 Battany MC (2012) Vineyard frost protection with upward-blowing wind machines. Agric
530 For Meteorol 157: 39–48

531 Blennow K (1998) Modelling minimum air temperature in partially and clear felled forests.
532 Agric For Meteorol 91: 223–235

533 Blennow K, Persson P (1998) Modelling local-scale frost variations using mobile
534 temperature measurements with a GIS. Agric For Meteorol 89: 59–71

535 Cavender-Bares J. (2005). Impacts of freezing on long distance transport in woody plants.
536 *Vascular transport in plants*, 401-424.

537 Cellier P (1984) Une méthode simple de prévision des températures de l'air et de la surface
538 du sol en conditions de gelées radiatives. Agronomie 4: 741–747

539 Cellier P (1993) An operational model for predicting minimum temperature near the soil
540 surface under sky conditions. J Appl Meteorol 32: 871–883

541 Charra-Vaskou K, Charrier G, Wortemann R, Beikircher B, Cochard H, Améglio T, Mayr
542 S (2012) Drought and frost resistance of trees: a comparison of four species at different sites
543 and altitudes. Ann For Sci 69: 325–333

544 Charra-Vaskou K, Badel E, Charrier G, Ponomarenko A, Bonhomme M, Foucat L, Mayr
545 S, Améglio T (2016) Cavitation and water fluxes driven by ice water potential in *Juglans*
546 *regia* during freeze–thaw cycles. J Exp Bot 67: 739–750
547 Charrier G, Cochard H, Améglio T (2013a) Evaluation of the impact of frost resistances on
548 potential altitudinal limit of trees. Tree Physiol 33: 891–902
549 Charrier G, Poirier M, Bonhomme M, Lacointe A, and Améglio T. (2013b). Frost
550 acclimation in different organs of walnut trees *Juglans regia* L.: How to link physiology and
551 modelling? Tree Physiology 33: 1229-1241.
552 Charrier G, Charra-Vaskou K, Kasuga J, Cochard H, Mayr S, Améglio T (2014a) Freeze-
553 thaw stress: effects of temperature on hydraulic conductivity and ultrasonic activity in ten
554 woody angiosperms. Plant Physiol 164: 992–998
555 Charrier G, Charra-Vaskou K, Legros B, Améglio T, Mayr S (2014b) Changes in
556 ultrasound velocity and attenuation indicate freezing of xylem sap. Agric For Meteorol 185:
557 20–25
558 Charrier G, Pramsohler M, Charra-Vaskou K, Saudreau M, Améglio T, Neuner G, Mayr S
559 (2015a) Ultrasonic emissions during ice nucleation and propagation in plant xylem. New
560 Phytol 207: 570–578
561 Charrier G, Ngao J, Saudreau M, Améglio T (2015b) Effects of environmental factors and
562 management practices on microclimate, winter physiology, and frost resistance in trees.
563 Front Plant Sci 6: 259
564 Christersson L (1978) The influence of photoperiod and temperature on the development
565 of frost hardiness in seedlings of *Pinus sylvestris* and *Picea abies*. Physiol Plant 44: 288–294
566 Cinotti B (1991) Recherche de propriétés intrinsèques du bois pouvant expliquer la
567 sensibilité à la gélivure de *Quercus petraea* (Liebl) et *Q. robur* (L). Ann For Sci 48: 453–
568 468

569 Daubenmire RF (1945) An improved type of precision dendrometer. Ecology 26: 97–98.
570 Dereuddre J, Gazeau C (1992) “Les végétaux et les très basses températures,” in Les
571 végétaux et le froid, ed. D. Côme (Paris: Hermann), 107–175
572 Deslauriers A, Rossi S, Anfodillo T (2007) Dendrometer and intra-annual tree growth:
573 what kind of information can be inferred? Dendrochronologia 25: 113–124
574 De Swaef T, De Schepper V, Vandegehuchte MW, Steppe K (2015) Stem diameter
575 variations as a versatile research tool in ecophysiology. Tree Physiol 35: 1047–1061
576 Dixon HH (1896) Transpiration into a saturated atmosphere. Proc R Ir Acad 4: 627–635
577 Hacker J, Neuner G (2007) Ice propagation in plants visualized at the tissue level by
578 infrared differential thermal analysis (IDTA). Tree Physiol 27: 1661–1670
579 Hansen J, Beck E (1988) Evidence for ideal and non-ideal equilibrium freezing of leaf
580 water in frost hardy ivy (*Hedera helix*) and winter barley (*Hordeum vulgare*). Bot Acta 101:
581 76–82
582 Hare DE, Sorensen CM (1987). The density of supercooled water. II. Bulk samples cooled
583 to the homogeneous nucleation limit. The Journal of chemical physics, 87: 4840-4845
584 Henson WR (1952) Chinook winds and red belt injury to lodgepole pine in the Rocky
585 mountains parks area of Canada. For Chron 28: 62–64
586 Holten V, Bertrand CE, Anisimov MA, Sengers JV. (2012) Thermodynamics of
587 supercooled water. The Journal of chemical physics, 136: 094507
588 Jordan DN, Smith WK (1994) Energy balance analysis of nighttime leaf temperatures and
589 frost formation in a sub alpine environment. Agric For Meteorol 71: 359–372
590 Kalyanasundaram P, Mukhopadhyay CK, Subba Rao SV (2007) Practical acoustic
591 emission. National certification board series, Indian Society for Non-Destructive Testing.
592 Alpha Science International, Oxford, UK

593 Kasuga J, Charrier G, Uemura M, Améglio T (2015) Characteristics of ultrasonic acoustic
594 emissions from walnut twigs during freeze–thaw-induced embolism formation. J Exp Bot
595 66: 1965–1975
596 Kikuta SB (2003) Ultrasound acoustic emissions from bark samples differing in anatomical
597 characteristics. Phyton, 43: 161-178
598 Kikuta SB, Richter H. (2003) Ultrasound acoustic emissions from freezing xylem. Plant,
599 Cell & Environment, 26: 383-388
600 Kubler H (1983) Mechanism of frost crack formation in trees - a review and synthesis. For
601 Sci 29: 559–568
602 Langer JS, Sekerka RF, Fujioka T (1978) Evidence for a universal law of dendritic growth
603 rates. J Cryst Growth 44: 414–418
604 Larcher W (1957) Frosttrocknis an der Waldgrenze und in der alpinen Zwergstrauchheide
605 auf dem Patscherkofel bei Innsbruck. Veröff Mus Ferdinandeum Innsbruck 37: 49–81
606 Larcher W (1963) Zur spätwinterlichen Erschwerung der Wasserbilanz von Holzpflanzen
607 an der Waldgrenze. Ber Nat Med Ver Innsbruck 53: 125–137
608 Larcher W (1977) Ergebnisse des IBP-Projekt „Zwergstrauchheide Patscherkofel“.
609 Springer, Berlin, Heidelberg, pp 301–371
610 Lemoine D, Granier A, Cochard H (1999) Mechanism of freeze-induced embolism in
611 *Fagus sylvatica* L. Trees 13, 206–210
612 Leuning R (1988) Leaf temperature during radiation frost. 2. A steady state theory. Agric
613 For Meteorol 42: 135–155
614 Leuning R, Cremer KW (1988) Leaf temperature during radiation frost. 1. Observations.
615 Agric For Meteorol 42: 121–133
616 Levitt JD (1958) Frost, drought and heat resistance. Protoplasmatologia 6: 1–87

617 Lindkvist L, Gustavsson T, Bogren J (2000) A frost assessment method for mountainous
618 areas. Agric For Meteorol 102: 51–67
619 Lintunen A, Hölttä T, Kulmala M (2013) Anatomical regulation of ice nucleation and
620 cavitation helps trees to survive freezing and drought stress. Scientific Reports 3: 203
621 Lintunen A, Paljakka T, Riikonen A, Lindén L, Lindfors L, Nikinmaa E, Hölttä T (2015)
622 Irreversible diameter change of wood segments correlates with other methods for estimating
623 frost tolerance of living cells in freeze-thaw experiment: a case study with seven urban tree
624 species in Helsinki. Ann For Sci 72: 1089–1098
625 Mayr S, Charra-Vaskou K (2007) Winter at the alpine timberline causes complex within-
626 tree patterns of water potential and embolism in *Picea abies*. Physiologia plantarum, 131:
627 131-139.
628 Mayr S, Sperry JS (2010) Freeze-thaw-induced embolism in *Pinus contorta*: centrifuge
629 experiments validate the 'thaw-expansion hypothesis' but conflict with ultrasonic emission
630 data. New Phytol 185: 1016–1024
631 Mayr S, Rosner S (2011) Cavitation in dehydrating xylem of *Picea abies*: energy
632 properties of ultrasonic emissions reflect tracheid dimensions. Tree Physiol 31: 59–67
633 Mayr S, Wolfschwenger M, Bauer H (2002) Winter-drought induced embolism in Norway
634 spruce (*Picea abies*) at the alpine timberline. Physiol Plant 115: 74–80
635 Mayr S, Gruber A, Bauer H (2003) Repeated freeze-thaw cycles induce embolism in
636 drought stressed conifers (Norway spruce, stone pine). Planta 217: 436–441
637 Mayr S, Wieser G, Bauer H (2006a) Xylem temperatures during winter in conifers at the
638 alpine timberline. Agric For Meteorol 137: 81–88
639 Mayr S, Hacke U, Schmid P, Schwienbacher F, Gruber A (2006b) Frost drought in
640 conifers at the alpine timberline: xylem dysfunction and adaptations. Ecology 87: 3175–
641 3185

642 Mayr S, Cochard H, Améglio T, Kikuta SB (2007) Embolism formation during freezing in
643 the wood of *Picea abies*. Plant Physiol 143: 60–67
644 Mayr S, Schmid P, Laur J, Rosner S, Charra-Vaskou K, Damon B, Hacke UG (2014)
645 Uptake of water via branches helps timberline conifers refill embolized xylem in late winter.
646 Plant Physiol 164: 1731–1740
647 Michaelis P (1934a) Ökologische Studien an der alpinen Baumgrenze. IV: Zur Kenntnis
648 des winterlichen Wasserhaushaltes. Jahrb Wiss Bot 80: 169–298
649 Michaelis P (1934b) Ökologische Studien an der alpinen Baumgrenze. V: Osmotischer
650 Wert und Wassergehalt während des winters in den verschiedenen Höhenlagen. Jahrb Wiss
651 Bot 80: 337–362
652 Milburn, J. A. (1966). The conduction of sap. *Planta*, *69*(1), 34-42.
653 Monteith JL, Unsworth MH. (eds) (1990) Principles of Environmental Physics. 2nd Ed.
654 London: Edward Arnold. 304 pp
655 Neuner G, Xu B, Hacker J (2010) Velocity and pattern of ice propagation and deep
656 supercooling in woody stems of *Castanea sativa*, *Morus nigra* and *Quercus robur* measured
657 by IDTA. Tree Physiol 30: 1037–1045
658 Nobel PS (1987) Principles underlying the prediction of temperature in plants, with special
659 reference to desert succulents. In Plants and Temperature Eds. S.I. Long, F.I. Woodward.
660 Society for Experimental Biology, Cambridge, pp 1–25
661 Nolf M, Creek D, Duursma R, Holtum J, Mayr S, Choat B (2015) Stem and leaf hydraulic
662 properties are finely coordinated in three tropical rainforest tree species. Plant Cell Environ
663 38: 2652–2661
664 Pearce RS (2001) Plant freezing and damage. Ann Bot 87: 417–424
665 Pittermann J, Sperry JS (2003) Tracheid diameter is the key trait determining the extent of
666 freezing-induced embolism in conifers. Tree Physiol, 23: 907-914

667 Pramsohler M, Hacker J, Neuner G (2012) Freezing pattern and frost killing temperature of
668 apple (*Malus domestica*) wood under controlled conditions and in nature. Tree Physiol 32:
669 819–828
670 Rauschenberger P, Criscione A, Eisenschmidt K, Kintea D, Jarkilic S, Tukovic Z, Roisman
671 IV, Weigand B, Tropea C (2013) Comparative assessment of volume-of-fluid and level-set
672 methods by relevance to dendritic ice growth in supercooled water. Comp Fluids 79: 44–52
673 Reineke LH (1932) A precision dendrometer. J For 30: 692–699
674 Repo T (1992) Seasonal changes of frost hardiness in *Picea abies* and *Pinus sylvestris* in
675 Finland. Can J For Res 22: 1949–1957
676 Robson DJ, McHardy WJ, Petty JA. (1988) Freezing in conifer xylem: II. Pit aspiration
677 and bubble formation. Journal of Experimental Botany, 1617-1621.
678 Ruelland E, Vaultier MN, Zachowski A, Hurry V (2009) Cold signalling and cold
679 acclimation in plants. Adv Bot Res 49: 35–150
680 Sakai A, Larcher W (1987) Frost survival of plants. Responses and adaptation to freezing
681 stress. In Ecological studies. Springer Verlag, Berlin, 321 pp
682 Sevanto S, Holbrook NM, Ball MC (2012) Freeze/thaw-induced embolism: probability of
683 critical bubble formation depends on speed of ice formation. Front Plant Sci 3: 107
684 Shibkov AA, Golovin YI, Zheltov MA, Korolev AA, Leonov AA (2003) Morphology
685 diagram of nonequilibrium patterns of ice crystals growing in supercooled water. Physica A
686 319: 65–79
687 Siminovitch D, Singh J, De La Roche IA (1978) Freezing behavior of free protoplasts of
688 winter rye. Cryobiology 15: 205–213
689 Snyder RL, Melo-Abreu JP (2005) Frost Protection: fundamentals, practice and economics,
690 Vol. 1 Food and Agriculture Organization of the United Nations, Rome. 240 pp

691 Sperry JS, Robson DG (2001) Xylem cavitation and freezing in conifers. In Colombo S,
692 Bigras F, eds, Conifer Cold Hardiness. Kluwer Academic Publishers, Dordrecht, The
693 Netherlands, pp 121–136
694 Sperry JS, Sullivan JEM (1992) Xylem embolism in response to freeze–thaw cycles and
695 water stress in ring-porous, diffuse-porous and conifer species. Plant Physiol 100: 605–613
696 Tappeiner U (1985) Bestandesstruktur, Mikroklima und Energiehaushalt einer naturnahen
697 Almweide und einerbegrünten Schipistenplanierung im Gasteiner Tal (Hohe Tauern).
698 Innsbruck.
699 Tranquillini W (1979) Physiological Ecology of the Alpine Timberline. Springer, Berlin.
700 137 pp
701 Tyree MT & Dixon MA (1983) Cavitation events in *Thuja occidentalis* L.? Utrasonic
702 acoustic emissions from the sapwood can be measured. Plant Physiology, 72: 1094-1099.
703 Uemura M, Tominaga Y, Nakagawara C, Shigematsu S, Minami A, Kawamura Y (2006)
704 Responses of the plasma membrane to low temperatures. Physiol Plant 126: 81–89
705 Vergeynst LL, Dierick M, Bogaerts JA, Cnudde V, Steppe K (2015) Cavitation: a blessing
706 in disguise? New method to establish vulnerability curves and assess hydraulic capacitance
707 of woody tissues. Tree Physiol 35: 400–409
708 Wardle P (1971) An explanation for alpine timberline. N Z J Bot. 9: 371–402
709 Winkel T, Lhomme JP, Nina Laura JP, Alcon CM, Del Castillo C, Rocheteau A (2009)
710 Assessing the protective effect of vertically heterogeneous canopies against radiative frost:
711 the case of quinoa on the Andean Altiplano. Agric For Meteorol 149: 1759–1768
712 Wisniewski M, Lindow SE, Ashworth EN (1997) Observations of ice nucleation and
713 propagation in plants using infrared video thermography. Plant Physiol 113: 327–334
714 Wolfe J, Bryant G (2001) Cellular cryobiology: thermodynamic and mechanical effects. Int
715 J Refrig 24: 438–450

716 Yelenosky G, Guy CL (1989) Freezing tolerance of citrus, spinach and petunia leaf tissue.
717 Osmotic adjustment and sensitivity to freeze induced cellular dehydration. Plant Physiol 89:
718 444–451
719 Zweifel R, Häsler R (2000) Frost-induced reversible shrinkage of bark of mature subalpine
720 conifers. Agricultural and Forest Meteorology 102: 213–222
721

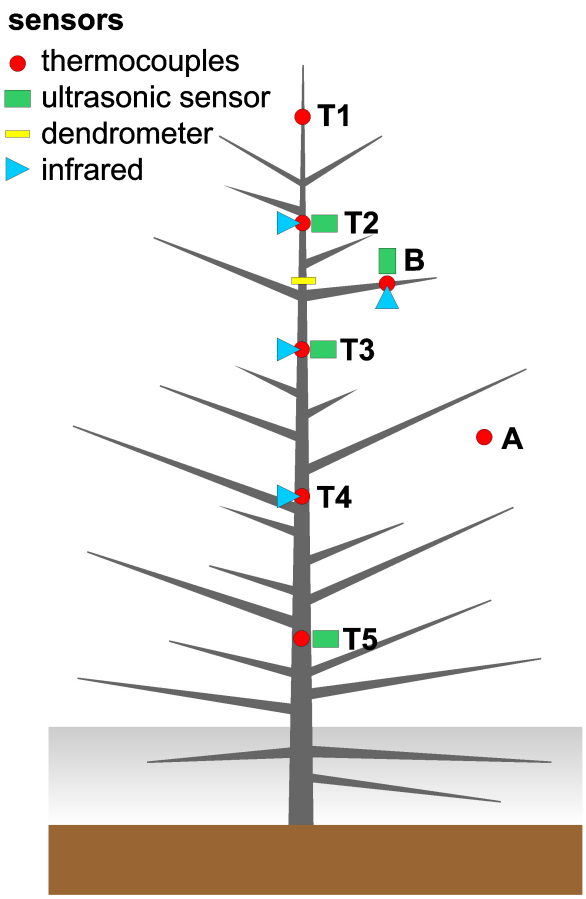

Figure 1. Measurement setup and sensor positions along a *Picea abies* tree.

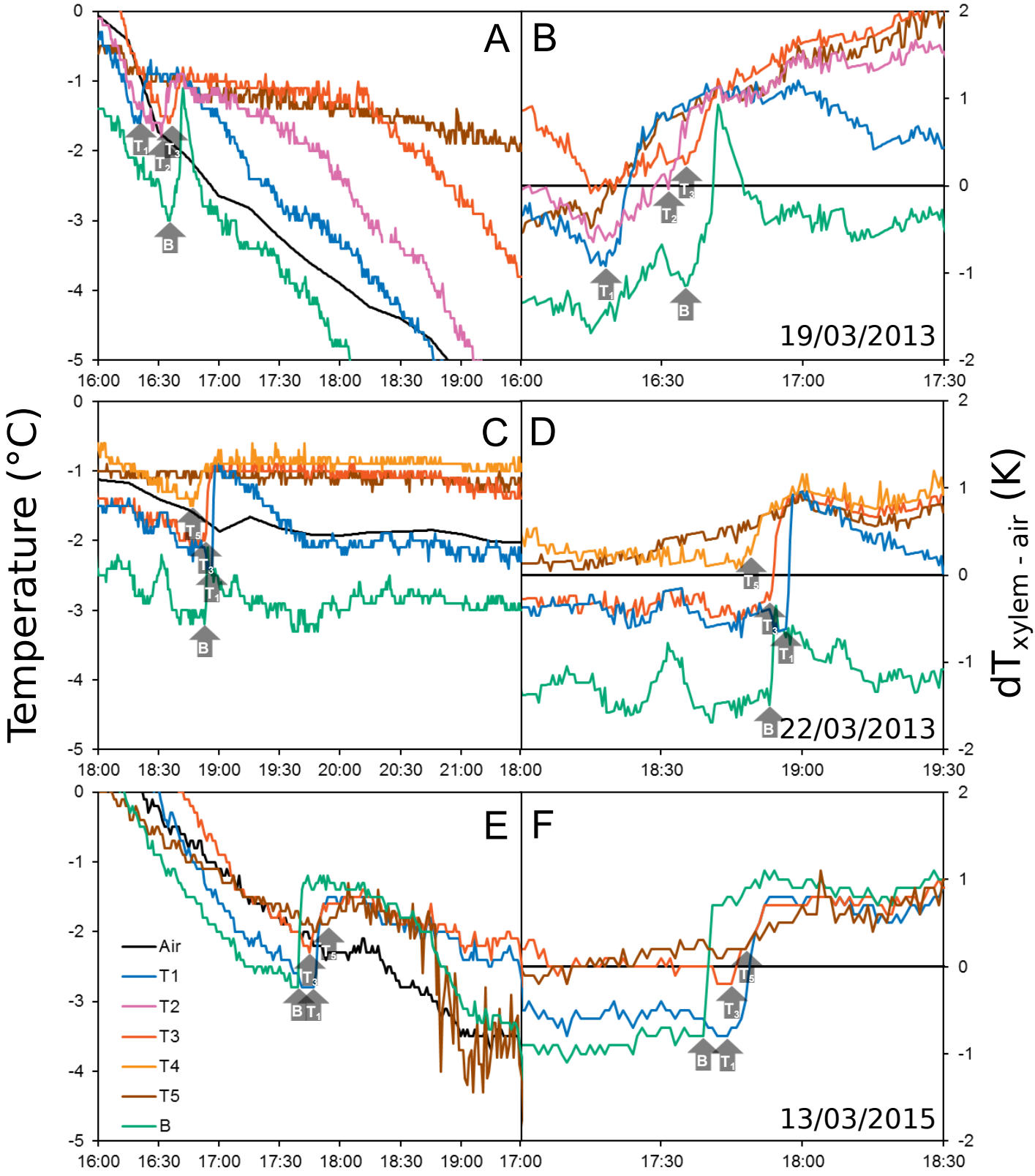

Figure 2. Freezing patterns as observed via freezing exotherms along a *Picea abies* tree growing at the alpine timberline after sunset using thermocouples inserted into the xylem. Left panels (A, C, E) show absolute temperatures during one evening. Right panels (B, D, F) present differential thermal analysis (xylem - air temperature) during the same freezing events. Arrows indicate the onset of exotherms at different sensor positions (B, T_1 - T_5) according to Fig. 1.

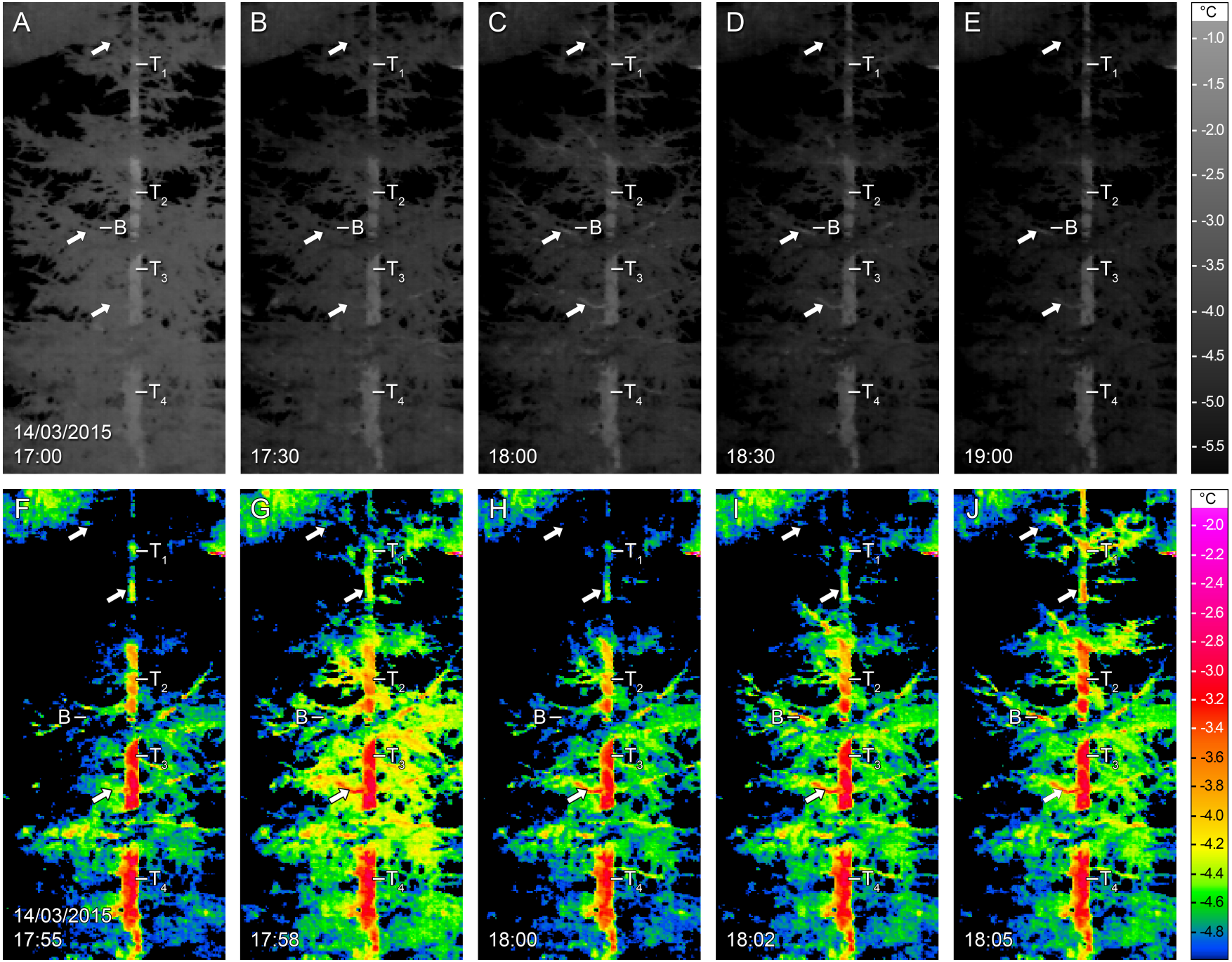

Figure 3. Spatial temperature patterns in a *Picea abies* tree growing at the alpine timberline at the time of freezing (after sunset; approx. 17:55) monitored via infrared imaging. Letters (B, T_1-T_4) indicate sensor positions (see Fig. 1), arrows indicate additional positions with very pronounced changes. Note different time scales in the upper vs. lower row. Upper grey panels (A) show temperature changes over two hours within the crown. Lower panels (B) illustrate the period when xylem exotherms were detected (17:55 to 18:05). This timeframe thus corresponds to the onset of the freezing, and areas with pronounced events where highlighted in the thermograms .

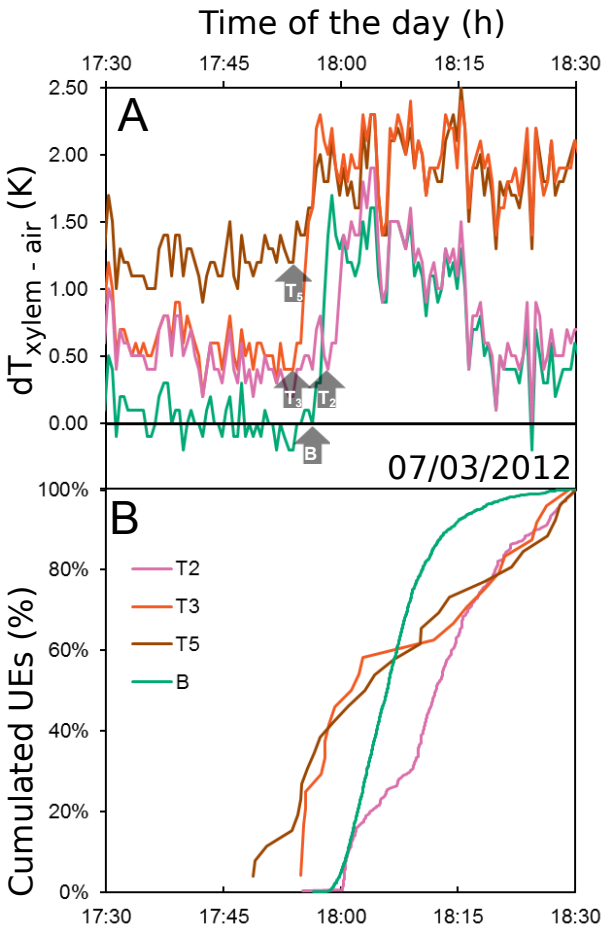

Figure 4. Sequence of freezing exotherms observed using thermocouples (differential thermal analysis, xylem - air temperature; A) and cumulated ultrasonic acoustic emissions (UEs; B) in a *Picea abies* tree during a freezing event. Arrows indicate the onset of exotherms at different sensor positions (B, T_2, T_3, T_5).

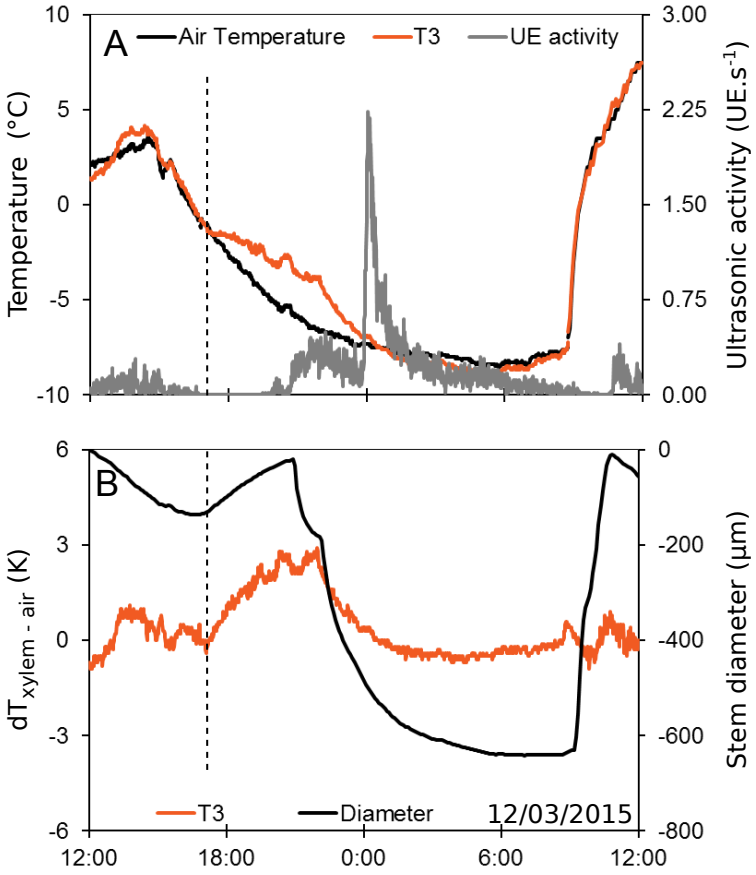

Figure 5. Ultrasonic activity (A) and stem diameter changes (B) in a *Picea abies* tree during a freezing event. Temperatures are given as absolute (T_3, Air; A) and differential (xylem - air temperature; B) values. Stem diameter is given as differential with respect to initial diameter (*i.e.* Day 1, 12:00) to highlight dynamic changes. Vertical dashed lines indicate the onset of exotherms as observed using thermocouple data.

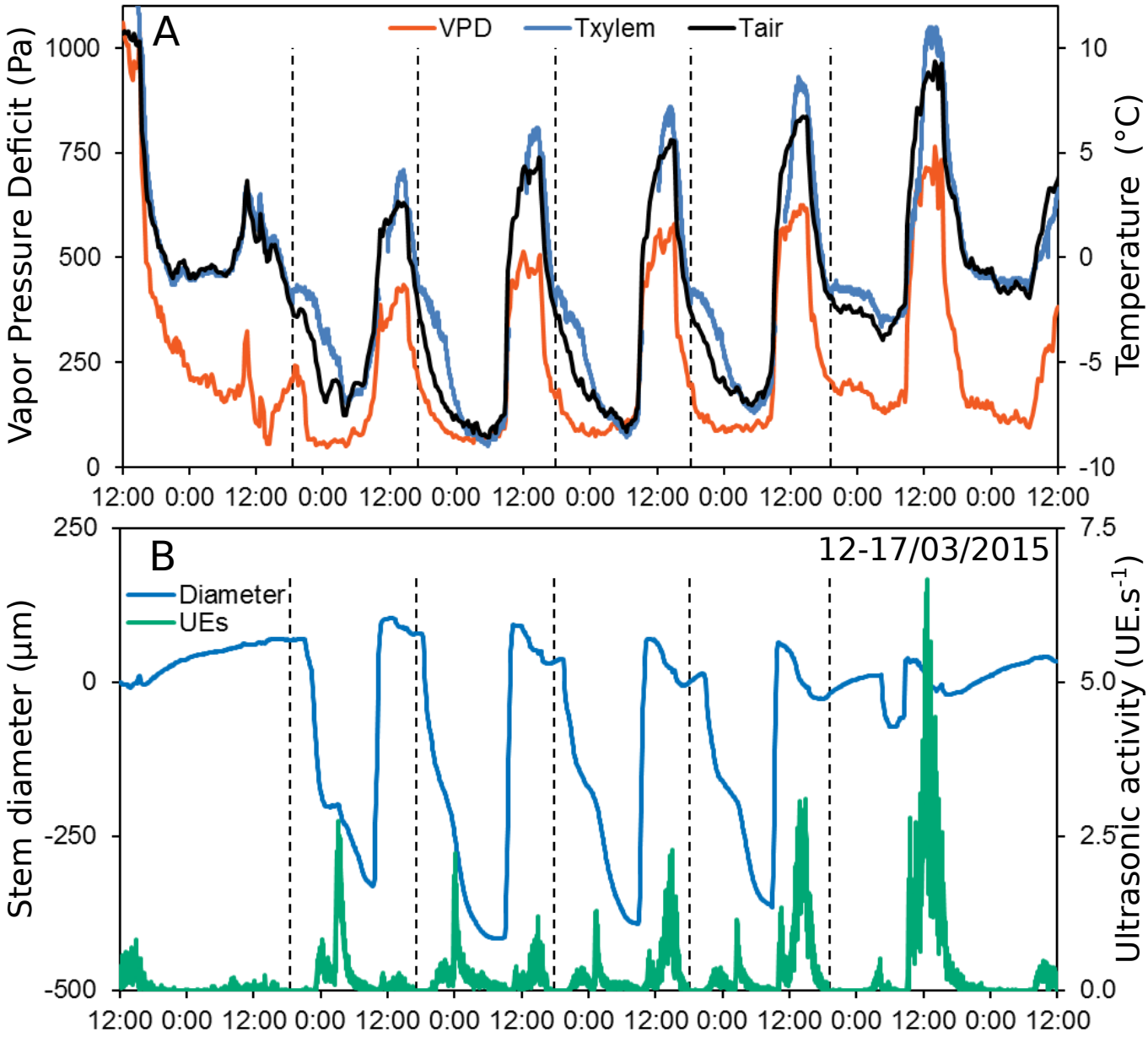

Figure 6. Diurnal sequences of environmental conditions (air and xylem temperature, vapor pressure deficit; A), stem diameter changes, and ultrasonic activity (B) in a *Picea abies* tree during six days with five freeze-thaw cycles. Stem diameter is given as differential with respect to initial diameter (*i.e.* Day 1, 12:00) to highlight dynamic changes. Vertical dashed lines indicate the onset of the freezing exotherms as observed by thermocouples.

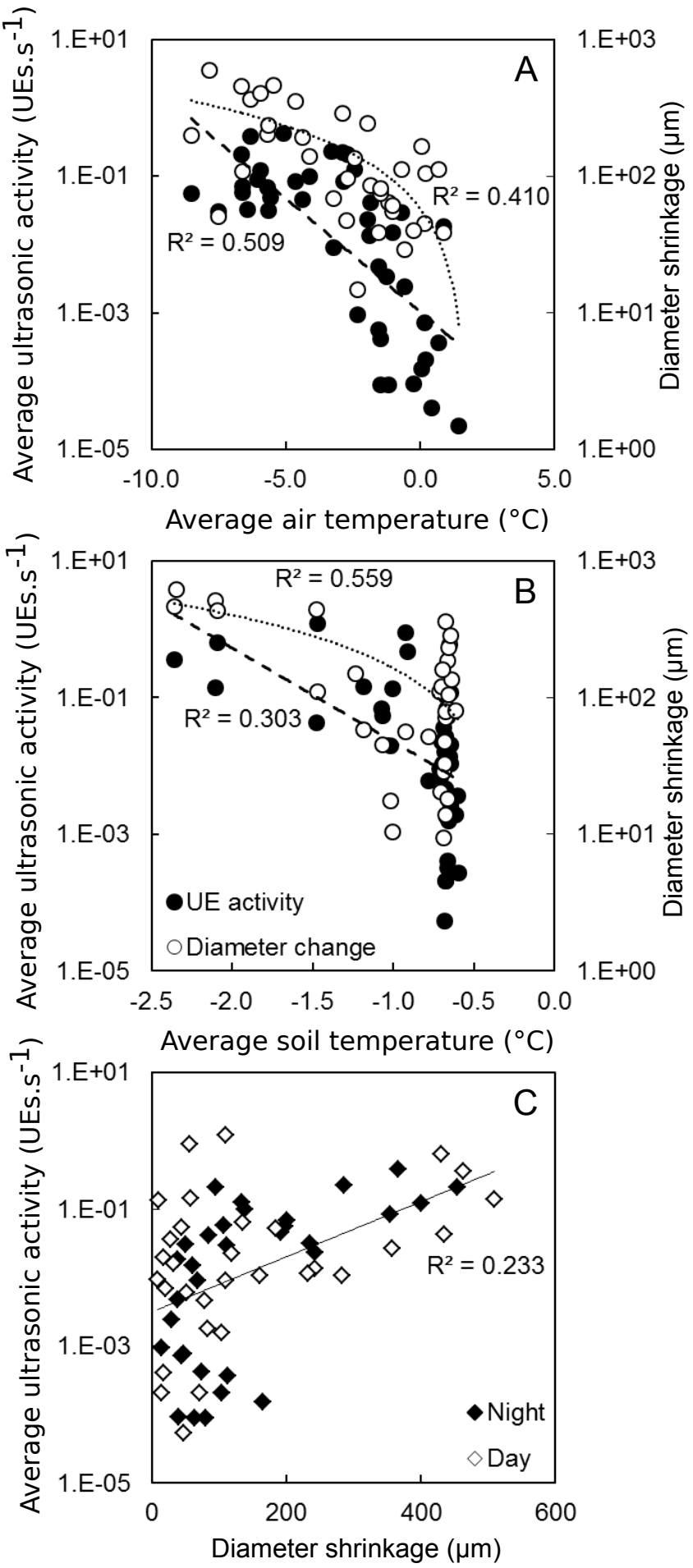

Figure 7. Average ultrasonic activity (filled dots) and diameter shrinkage (white dots) observed per night (net radiation < 10 $W.M^{-2}$) depending on average air temperature (A), or per day depending on average soil temperature (B). Average ultrasonic activities depending on diameter shrinkage (C) are presented with no significant difference between day (white diamonds) and night (filled diamonds). Note that y-scales are logarithmic. R^2 values apply to exponential (UE activities) or linear fits (diameter shrinkage).

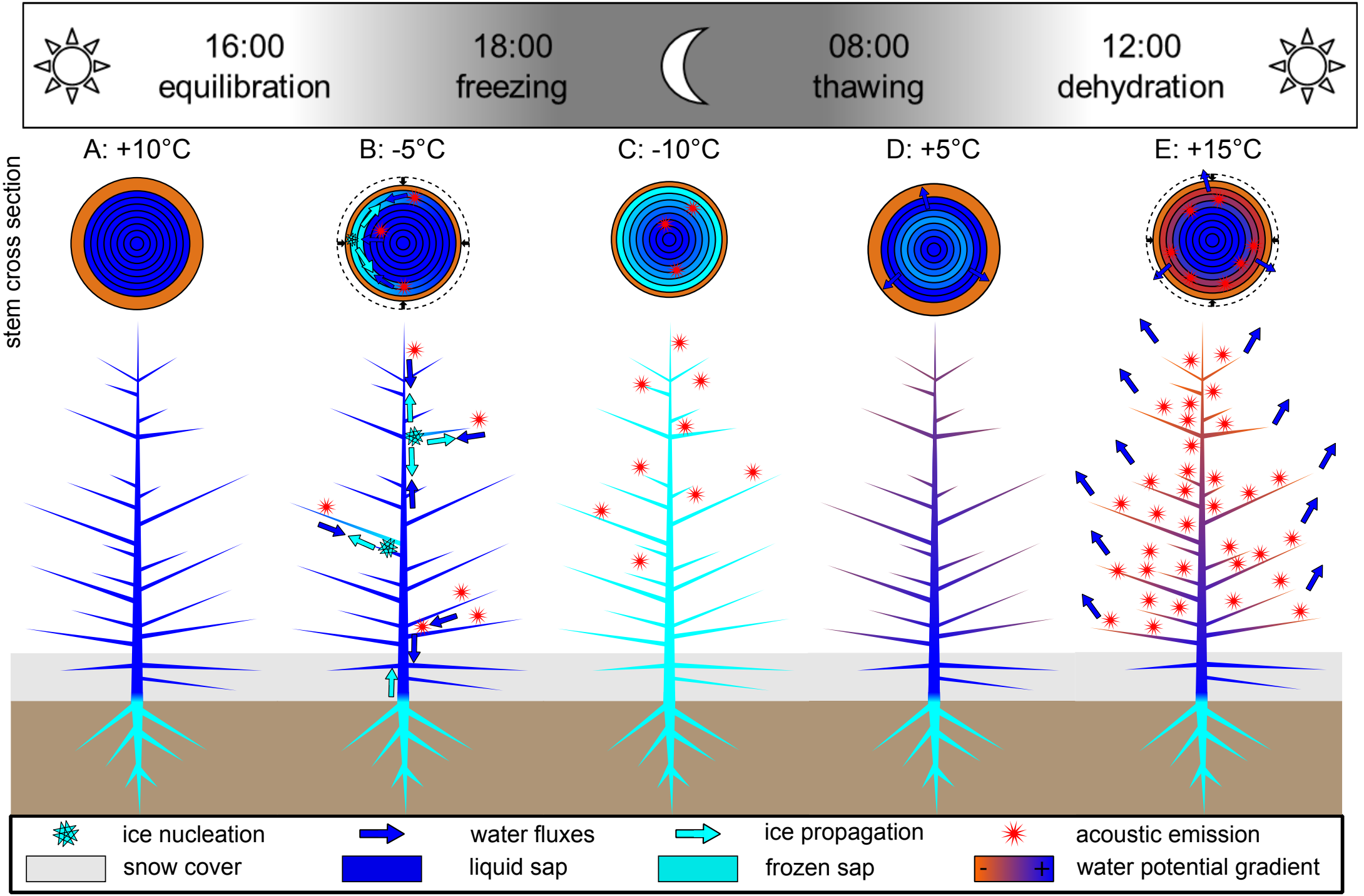

Figure 8. Generalized scheme of observed patterns and underlying water fluxes in a *Picea abies* tree during a freeze-thaw cycle in late winter. Initial equilibrated state (A), ice nucleation and propagation with associated water fluxes, stem shrinkage and ultrasonic emissions (B), ultrasonic activity after exotherm dissipation (C), stem diameter increase and developing water potential gradient during thawing (D), and stem shrinkage and high ultrasonic activity during daytime transpiration with frozen soil (E).

Parsed Citations

Améglio T, Cochard H, Ewers F (2001) Stem diameter variations and cold hardiness in walnut trees. J Exp Bot 52: 2135-2142
Pubmed: Author and Title
CrossRef: Author and Title
Google Scholar: Author Only Title Only Author and Title

Asahina E (1956) The freezing process of plant cell. Contrib Inst Low Temp Sci Hokkaido Univ 10: 83-126
Pubmed: Author and Title
CrossRef: Author and Title
Google Scholar: Author Only Title Only Author and Title

Ball MC, Canny MJ, Huang CX, Egerton JJG, Wolfe J (2006) Freeze/thaw-induced embolism depends on nadir temperature: the heterogeneous hydration hypothesis. Plant Cell Environ 29: 729-745
Pubmed: Author and Title
CrossRef: Author and Title
Google Scholar: Author Only Title Only Author and Title

Battany MC (2012) Vineyard frost protection with upward-blowing wind machines. Agric For Meteorol 157: 39-48
Pubmed: Author and Title
CrossRef: Author and Title
Google Scholar: Author Only Title Only Author and Title

Blennow K (1998) Modelling minimum air temperature in partially and clear felled forests. Agric For Meteorol 91: 223-235
Pubmed: Author and Title
CrossRef: Author and Title
Google Scholar: Author Only Title Only Author and Title

Blennow K, Persson P (1998) Modelling local-scale frost variations using mobile temperature measurements with a GIS. Agric For Meteorol 89: 59-71
Pubmed: Author and Title
CrossRef: Author and Title
Google Scholar: Author Only Title Only Author and Title

Cavender-Bares J. (2005). Impacts of freezing on long distance transport in woody plants. Vascular transport in plants, 401-424.
Pubmed: Author and Title
CrossRef: Author and Title
Google Scholar: Author Only Title Only Author and Title

Cellier P (1984) Une méthode simple de prévision des températures de l'air et de la surface du sol en conditions de gelées radiatives. Agronomie 4: 741-747
Pubmed: Author and Title
CrossRef: Author and Title
Google Scholar: Author Only Title Only Author and Title

Cellier P (1993) An operational model for predicting minimum temperature near the soil surface under sky conditions. J Appl Meteorol 32: 871-883
Pubmed: Author and Title
CrossRef: Author and Title
Google Scholar: Author Only Title Only Author and Title

Charra-Vaskou K, Charrier G, Wortemann R, Beikircher B, Cochard H, Améglio T, Mayr S (2012) Drought and frost resistance of trees: a comparison of four species at different sites and altitudes. Ann For Sci 69: 325-333
Pubmed: Author and Title
CrossRef: Author and Title
Google Scholar: Author Only Title Only Author and Title

Charra-Vaskou K, Badel E, Charrier G, Ponomarenko A, Bonhomme M, Foucat L, Mayr S, Améglio T (2016) Cavitation and water fluxes driven by ice water potential in Juglans regia during freeze-thaw cycles. J Exp Bot 67: 739-750
Pubmed: Author and Title
CrossRef: Author and Title
Google Scholar: Author Only Title Only Author and Title

Charrier G, Cochard H, Améglio T (2013a) Evaluation of the impact of frost resistances on potential altitudinal limit of trees. Tree Physiol 33: 891-902
Pubmed: Author and Title
CrossRef: Author and Title
Google Scholar: Author Only Title Only Author and Title

Charrier G, Poirier M, Bonhomme M, Lacointe A, and Améglio T. (2013b). Frost acclimation in different organs of walnut trees Juglans regia L.: How to link physiology and modelling? Tree Physiology 33: 1229-1241.
Pubmed: Author and Title
CrossRef: Author and Title
Google Scholar: Author Only Title Only Author and Title

Charrier G, Charra-Vaskou K, Kasuga J, Cochard H, Mayr S, Améglio T (2014a) Freeze-thaw stress: effects of temperature on hydraulic conductivity and ultrasonic activity in ten woody angiosperms. Plant Physiol 164: 992-998
Pubmed: Author and Title
CrossRef: Author and Title
Google Scholar: Author Only Title Only Author and Title

Charrier G, Charra-Vaskou K, Legros B, Améglio T, Mayr S (2014b) Changes in ultrasound velocity and attenuation indicate freezing of xylem sap. Agric For Meteorol 185: 20-25
Pubmed: Author and Title
CrossRef: Author and Title
Google Scholar: Author Only Title Only Author and Title

Charrier G, Pramsohler M, Charra-Vaskou K, Saudreau M, Améglio T, Neuner G, Mayr S (2015a) Ultrasonic emissions during ice nucleation and propagation in plant xylem. New Phytol 207: 570-578
Pubmed: Author and Title
CrossRef: Author and Title
Google Scholar: Author Only Title Only Author and Title

Charrier G, Ngao J, Saudreau M, Améglio T (2015b) Effects of environmental factors and management practices on microclimate, winter physiology, and frost resistance in trees. Front Plant Sci 6: 259
Pubmed: Author and Title
CrossRef: Author and Title
Google Scholar: Author Only Title Only Author and Title

Christersson L (1978) The influence of photoperiod and temperature on the development of frost hardiness in seedlings of Pinus sylvestris and Picea abies. Physiol Plant 44: 288-294
Pubmed: Author and Title
CrossRef: Author and Title
Google Scholar: Author Only Title Only Author and Title

Cinotti B (1991) Recherche de propriétés intrinsèques du bois pouvant expliquer la sensibilité à la gélivure de Quercus petraea (Liebl) et Q. robur (L). Ann For Sci 48: 453-468
Pubmed: Author and Title
CrossRef: Author and Title
Google Scholar: Author Only Title Only Author and Title

Daubenmire RF (1945) An improved type of precision dendrometer. Ecology 26: 97-98.
Pubmed: Author and Title
CrossRef: Author and Title
Google Scholar: Author Only Title Only Author and Title

Dereuddre J, Gazeau C (1992) "Les végétaux et les très basses températures," in Les végétaux et le froid, ed. D. Côme (Paris: Hermann), 107-175
Pubmed: Author and Title
CrossRef: Author and Title
Google Scholar: Author Only Title Only Author and Title

Deslauriers A, Rossi S, Anfodillo T (2007) Dendrometer and intra-annual tree growth: what kind of information can be inferred? Dendrochronologia 25: 113-124
Pubmed: Author and Title
CrossRef: Author and Title
Google Scholar: Author Only Title Only Author and Title

De Swaef T, De Schepper V, Vandegehuchte MW, Steppe K (2015) Stem diameter variations as a versatile research tool in ecophysiology. Tree Physiol 35: 1047-1061
Pubmed: Author and Title
CrossRef: Author and Title
Google Scholar: Author Only Title Only Author and Title

Dixon HH (1896) Transpiration into a saturated atmosphere. Proc R Ir Acad 4: 627-635
Pubmed: Author and Title
CrossRef: Author and Title
Google Scholar: Author Only Title Only Author and Title

Hacker J, Neuner G (2007) Ice propagation in plants visualized at the tissue level by infrared differential thermal analysis (IDTA). Tree Physiol 27: 1661-1670
Pubmed: Author and Title
CrossRef: Author and Title
Google Scholar: Author Only Title Only Author and Title

Hansen J, Beck E (1988) Evidence for ideal and non-ideal equilibrium freezing of leaf water in frost hardy ivy (Hedera helix) and winter barley (Hordeum vulgare). Bot Acta 101: 76-82
Pubmed: Author and Title
CrossRef: Author and Title
Google Scholar: Author Only Title Only Author and Title

Hare DE, Sorensen CM (1987). The density of supercooled water. II. Bulk samples cooled to the homogeneous nucleation limit. The Journal of chemical physics, 87: 4840-4845
Pubmed: Author and Title
CrossRef: Author and Title
Google Scholar: Author Only Title Only Author and Title

Henson WR (1952) Chinook winds and red belt injury to lodgepole pine in the Rocky mountains parks area of Canada. For Chron 28: 62-64
Pubmed: Author and Title
CrossRef: Author and Title

Google Scholar: Author Only Title Only Author and Title

Holten V, Bertrand CE, Anisimov MA, Sengers JV. (2012) Thermodynamics of supercooled water. The Journal of chemical physics, 136: 094507
Pubmed: Author and Title
CrossRef: Author and Title
Google Scholar: Author Only Title Only Author and Title

Jordan DN, Smith WK (1994) Energy balance analysis of nighttime leaf temperatures and frost formation in a sub alpine environment. Agric For Meteorol 71: 359-372
Pubmed: Author and Title
CrossRef: Author and Title
Google Scholar: Author Only Title Only Author and Title

Kalyanasundaram P, Mukhopadhyay CK, Subba Rao SV (2007) Practical acoustic emission. National certification board series, Indian Society for Non-Destructive Testing. Alpha Science International, Oxford, UK
Pubmed: Author and Title
CrossRef: Author and Title
Google Scholar: Author Only Title Only Author and Title

Kasuga J, Charrier G, Uemura M, Améglio T (2015) Characteristics of ultrasonic acoustic emissions from walnut twigs during freeze-thaw-induced embolism formation. J Exp Bot 66: 1965-1975
Pubmed: Author and Title
CrossRef: Author and Title
Google Scholar: Author Only Title Only Author and Title

Kikuta SB (2003) Ultrasound acoustic emissions from bark samples differing in anatomical characteristics. Phyton, 43: 161-178
Pubmed: Author and Title
CrossRef: Author and Title
Google Scholar: Author Only Title Only Author and Title

Kikuta SB, Richter H. (2003) Ultrasound acoustic emissions from freezing xylem. Plant, Cell & Environment, 26: 383-388
Pubmed: Author and Title
CrossRef: Author and Title
Google Scholar: Author Only Title Only Author and Title

Kubler H (1983) Mechanism of frost crack formation in trees - a review and synthesis. For Sci 29: 559-568
Pubmed: Author and Title
CrossRef: Author and Title
Google Scholar: Author Only Title Only Author and Title

Langer JS, Sekerka RF, Fujioka T (1978) Evidence for a universal law of dendritic growth rates. J Cryst Growth 44: 414-418
Pubmed: Author and Title
CrossRef: Author and Title
Google Scholar: Author Only Title Only Author and Title

Larcher W (1957) Frosttrocknis an der Waldgrenze und in der alpinen Zwergstrauchheide auf dem Patscherkofel bei Innsbruck. Veröff Mus Ferdinandeum Innsbruck 37: 49-81
Pubmed: Author and Title
CrossRef: Author and Title
Google Scholar: Author Only Title Only Author and Title

Larcher W (1963) Zur spätwinterlichen Erschwerung der Wasserbilanz von Holzpflanzen an der Waldgrenze. Ber Nat Med Ver Innsbruck 53: 125-137
Pubmed: Author and Title
CrossRef: Author and Title
Google Scholar: Author Only Title Only Author and Title

Larcher W (1977) Ergebnisse des IBP-Projekt „Zwergstrauchheide Patscherkofel". Springer, Berlin, Heidelberg, pp 301-371
Pubmed: Author and Title
CrossRef: Author and Title
Google Scholar: Author Only Title Only Author and Title

Lemoine D, Granier A, Cochard H (1999) Mechanism of freeze-induced embolism in Fagus sylvatica L. Trees 13, 206-210
Pubmed: Author and Title
CrossRef: Author and Title
Google Scholar: Author Only Title Only Author and Title

Leuning R (1988) Leaf temperature during radiation frost. 2. A steady state theory. Agric For Meteorol 42: 135-155
Pubmed: Author and Title
CrossRef: Author and Title
Google Scholar: Author Only Title Only Author and Title

Leuning R, Cremer KW (1988) Leaf temperature during radiation frost. 1. Observations. Agric For Meteorol 42: 121-133
Pubmed: Author and Title
CrossRef: Author and Title
Google Scholar: Author Only Title Only Author and Title

Levitt JD (1958) Frost, drought and heat resistance. Protoplasmatologia 6: 1-87
Pubmed: Author and Title
CrossRef: Author and Title

Google Scholar: Author Only Title Only Author and Title

Lindkvist L, Gustavsson T, Bogren J (2000) A frost assessment method for mountainous areas. Agric For Meteorol 102: 51-67
Pubmed: Author and Title
CrossRef: Author and Title
Google Scholar: Author Only Title Only Author and Title

Lintunen A, Hölttä T, Kulmala M (2013) Anatomical regulation of ice nucleation and cavitation helps trees to survive freezing and drought stress. Scientific Reports 3: 203
Pubmed: Author and Title
CrossRef: Author and Title
Google Scholar: Author Only Title Only Author and Title

Lintunen A, Paljakka T, Riikonen A, Lindén L, Lindfors L, Nikinmaa E, Hölttä T (2015) Irreversible diameter change of wood segments correlates with other methods for estimating frost tolerance of living cells in freeze-thaw experiment: a case study with seven urban tree species in Helsinki. Ann For Sci 72: 1089-1098
Pubmed: Author and Title
CrossRef: Author and Title
Google Scholar: Author Only Title Only Author and Title

Mayr S, Charra-Vaskou K (2007) Winter at the alpine timberline causes complex within-tree patterns of water potential and embolism in Picea abies. Physiologia plantarum, 131: 131-139.
Pubmed: Author and Title
CrossRef: Author and Title
Google Scholar: Author Only Title Only Author and Title

Mayr S, Sperry JS (2010) Freeze-thaw-induced embolism in Pinus contorta: centrifuge experiments validate the 'thaw-expansion hypothesis' but conflict with ultrasonic emission data. New Phytol 185: 1016-1024
Pubmed: Author and Title
CrossRef: Author and Title
Google Scholar: Author Only Title Only Author and Title

Mayr S, Rosner S (2011) Cavitation in dehydrating xylem of Picea abies: energy properties of ultrasonic emissions reflect tracheid dimensions. Tree Physiol 31: 59-67
Pubmed: Author and Title
CrossRef: Author and Title
Google Scholar: Author Only Title Only Author and Title

Mayr S, Wolfschwenger M, Bauer H (2002) Winter-drought induced embolism in Norway spruce (Picea abies) at the alpine timberline. Physiol Plant 115: 74-80
Pubmed: Author and Title
CrossRef: Author and Title
Google Scholar: Author Only Title Only Author and Title

Mayr S, Gruber A, Bauer H (2003) Repeated freeze-thaw cycles induce embolism in drought stressed conifers (Norway spruce, stone pine). Planta 217: 436-441
Pubmed: Author and Title
CrossRef: Author and Title
Google Scholar: Author Only Title Only Author and Title

Mayr S, Wieser G, Bauer H (2006a) Xylem temperatures during winter in conifers at the alpine timberline. Agric For Meteorol 137: 81-88
Pubmed: Author and Title
CrossRef: Author and Title
Google Scholar: Author Only Title Only Author and Title

Mayr S, Hacke U, Schmid P, Schwienbacher F, Gruber A (2006b) Frost drought in conifers at the alpine timberline: xylem dysfunction and adaptations. Ecology 87: 3175-3185
Pubmed: Author and Title
CrossRef: Author and Title
Google Scholar: Author Only Title Only Author and Title

Mayr S, Cochard H, Améglio T, Kikuta SB (2007) Embolism formation during freezing in the wood of Picea abies. Plant Physiol 143: 60-67
Pubmed: Author and Title
CrossRef: Author and Title
Google Scholar: Author Only Title Only Author and Title

Mayr S, Schmid P, Laur J, Rosner S, Charra-Vaskou K, Damon B, Hacke UG (2014) Uptake of water via branches helps timberline conifers refill embolized xylem in late winter. Plant Physiol 164: 1731-1740
Pubmed: Author and Title
CrossRef: Author and Title
Google Scholar: Author Only Title Only Author and Title

Michaelis P (1934a) Ökologische Studien an der alpinen Baumgrenze. IV: Zur Kenntnis des winterlichen Wasserhaushaltes. Jahrb Wiss Bot 80: 169-298
Pubmed: Author and Title
CrossRef: Author and Title
Google Scholar: Author Only Title Only Author and Title

Michaelis P (1934b) Ökologische Studien an der alpinen Baumgrenze. V: Osmotischer Wert und Wassergehalt während des

winters in den verschiedenen Höhenlagen. Jahrb Wiss Bot 80: 337-362
Pubmed: Author and Title
CrossRef: Author and Title
Google Scholar: Author Only Title Only Author and Title

Milburn, J. A. (1966). The conduction of sap. Planta, 69(1), 34-42.
Pubmed: Author and Title
CrossRef: Author and Title
Google Scholar: Author Only Title Only Author and Title

Monteith JL, Unsworth MH. (eds) (1990) Principles of Environmental Physics. 2nd Ed. London: Edward Arnold. 304 pp
Pubmed: Author and Title
CrossRef: Author and Title
Google Scholar: Author Only Title Only Author and Title

Neuner G, Xu B, Hacker J (2010) Velocity and pattern of ice propagation and deep supercooling in woody stems of Castanea sativa, Morus nigra and Quercus robur measured by IDTA. Tree Physiol 30: 1037-1045
Pubmed: Author and Title
CrossRef: Author and Title
Google Scholar: Author Only Title Only Author and Title

Nobel PS (1987) Principles underlying the prediction of temperature in plants, with special reference to desert succulents. In Plants and Temperature Eds. S.I. Long, F.I. Woodward. Society for Experimental Biology, Cambridge, pp 1-25
Pubmed: Author and Title
CrossRef: Author and Title
Google Scholar: Author Only Title Only Author and Title

Nolf M, Creek D, Duursma R, Holtum J, Mayr S, Choat B (2015) Stem and leaf hydraulic properties are finely coordinated in three tropical rainforest tree species. Plant Cell Environ 38: 2652-2661
Pubmed: Author and Title
CrossRef: Author and Title
Google Scholar: Author Only Title Only Author and Title

Pearce RS (2001) Plant freezing and damage. Ann Bot 87: 417-424
Pubmed: Author and Title
CrossRef: Author and Title
Google Scholar: Author Only Title Only Author and Title

Pittermann J, Sperry JS (2003) Tracheid diameter is the key trait determining the extent of freezing-induced embolism in conifers. Tree Physiol, 23: 907-914
Pubmed: Author and Title
CrossRef: Author and Title
Google Scholar: Author Only Title Only Author and Title

Pramsohler M, Hacker J, Neuner G (2012) Freezing pattern and frost killing temperature of apple (Malus domestica) wood under controlled conditions and in nature. Tree Physiol 32: 819-828
Pubmed: Author and Title
CrossRef: Author and Title
Google Scholar: Author Only Title Only Author and Title

Rauschenberger P, Criscione A, Eisenschmidt K, Kintea D, Jarkilic S, Tukovic Z, Roisman IV, Weigand B, Tropea C (2013) Comparative assessment of volume-of-fluid and level-set methods by relevance to dendritic ice growth in supercooled water. Comp Fluids 79: 44-52
Pubmed: Author and Title
CrossRef: Author and Title
Google Scholar: Author Only Title Only Author and Title

Reineke LH (1932) A precision dendrometer. J For 30: 692-699
Pubmed: Author and Title
CrossRef: Author and Title
Google Scholar: Author Only Title Only Author and Title

Repo T (1992) Seasonal changes of frost hardiness in Picea abies and Pinus sylvestris in Finland. Can J For Res 22: 1949-1957
Pubmed: Author and Title
CrossRef: Author and Title
Google Scholar: Author Only Title Only Author and Title

Robson DJ, McHardy WJ, Petty JA. (1988) Freezing in conifer xylem: II. Pit aspiration and bubble formation. Journal of Experimental Botany, 1617-1621.
Pubmed: Author and Title
CrossRef: Author and Title
Google Scholar: Author Only Title Only Author and Title

Ruelland E, Vaultier MN, Zachowski A, Hurry V (2009) Cold signalling and cold acclimation in plants. Adv Bot Res 49: 35-150
Pubmed: Author and Title
CrossRef: Author and Title
Google Scholar: Author Only Title Only Author and Title

Sakai A, Larcher W (1987) Frost survival of plants. Responses and adaptation to freezing stress. In Ecological studies. Springer Verlag, Berlin, 321 pp
Pubmed: Author and Title

CrossRef: Author and Title
Google Scholar: Author Only Title Only Author and Title

Sevanto S, Holbrook NM, Ball MC (2012) Freeze/thaw-induced embolism: probability of critical bubble formation depends on speed of ice formation. Front Plant Sci 3: 107
Pubmed: Author and Title
CrossRef: Author and Title
Google Scholar: Author Only Title Only Author and Title

Shibkov AA, Golovin YI, Zheltov MA, Korolev AA, Leonov AA (2003) Morphology diagram of nonequilibrium patterns of ice crystals growing in supercooled water. Physica A 319: 65-79
Pubmed: Author and Title
CrossRef: Author and Title
Google Scholar: Author Only Title Only Author and Title

Siminovitch D, Singh J, De La Roche IA (1978) Freezing behavior of free protoplasts of winter rye. Cryobiology 15: 205-213
Pubmed: Author and Title
CrossRef: Author and Title
Google Scholar: Author Only Title Only Author and Title

Snyder RL, Melo-Abreu JP (2005) Frost Protection: fundamentals, practice and economics, Vol. 1 Food and Agriculture Organization of the United Nations, Rome. 240 pp
Pubmed: Author and Title
CrossRef: Author and Title
Google Scholar: Author Only Title Only Author and Title

Sperry JS, Robson DG (2001) Xylem cavitation and freezing in conifers. In Colombo S, Bigras F, eds, Conifer Cold Hardiness. Kluwer Academic Publishers, Dordrecht, The Netherlands, pp 121-136
Pubmed: Author and Title
CrossRef: Author and Title
Google Scholar: Author Only Title Only Author and Title

Sperry JS, Sullivan JEM (1992) Xylem embolism in response to freeze-thaw cycles and water stress in ring-porous, diffuse-porous and conifer species. Plant Physiol 100: 605-613
Pubmed: Author and Title
CrossRef: Author and Title
Google Scholar: Author Only Title Only Author and Title

Tappeiner U (1985) Bestandesstruktur, Mikroklima und Energiehaushalt einer naturnahen Almweide und einerbegrünten Schipistenplanierung im Gasteiner Tal (Hohe Tauern). Innsbruck.
Pubmed: Author and Title
CrossRef: Author and Title
Google Scholar: Author Only Title Only Author and Title

Tranquillini W (1979) Physiological Ecology of the Alpine Timberline. Springer, Berlin. 137 pp
Pubmed: Author and Title
CrossRef: Author and Title
Google Scholar: Author Only Title Only Author and Title

Tyree MT & Dixon MA (1983) Cavitation events in Thuja occidentalis L.? Utrasonic acoustic emissions from the sapwood can be measured. Plant Physiology, 72: 1094-1099.
Pubmed: Author and Title
CrossRef: Author and Title
Google Scholar: Author Only Title Only Author and Title

Uemura M, Tominaga Y, Nakagawara C, Shigematsu S, Minami A, Kawamura Y (2006) Responses of the plasma membrane to low temperatures. Physiol Plant 126: 81-89
Pubmed: Author and Title
CrossRef: Author and Title
Google Scholar: Author Only Title Only Author and Title

Vergeynst LL, Dierick M, Bogaerts JA, Cnudde V, Steppe K (2015) Cavitation: a blessing in disguise? New method to establish vulnerability curves and assess hydraulic capacitance of woody tissues. Tree Physiol 35: 400-409
Pubmed: Author and Title
CrossRef: Author and Title
Google Scholar: Author Only Title Only Author and Title

Wardle P (1971) An explanation for alpine timberline. N Z J Bot. 9: 371-402
Pubmed: Author and Title
CrossRef: Author and Title
Google Scholar: Author Only Title Only Author and Title

Winkel T, Lhomme JP, Nina Laura JP, Alcon CM, Del Castillo C, Rocheteau A (2009) Assessing the protective effect of vertically heterogeneous canopies against radiative frost: the case of quinoa on the Andean Altiplano. Agric For Meteorol 149: 1759-1768
Pubmed: Author and Title
CrossRef: Author and Title
Google Scholar: Author Only Title Only Author and Title

Wisniewski M, Lindow SE, Ashworth EN (1997) Observations of ice nucleation and propagation in plants using infrared video thermography. Plant Physiol 113: 327-334
Pubmed: Author and Title

CrossRef: Author and Title
Google Scholar: Author Only Title Only Author and Title

Wolfe J, Bryant G (2001) Cellular cryobiology: thermodynamic and mechanical effects. Int J Refrig 24: 438-450
Pubmed: Author and Title
CrossRef: Author and Title
Google Scholar: Author Only Title Only Author and Title

Yelenosky G, Guy CL (1989) Freezing tolerance of citrus, spinach and petunia leaf tissue. Osmotic adjustment and sensitivity to freeze induced cellular dehydration. Plant Physiol 89: 444-451
Pubmed: Author and Title
CrossRef: Author and Title
Google Scholar: Author Only Title Only Author and Title

Zweifel R, Häsler R (2000) Frost-induced reversible shrinkage of bark of mature subalpine conifers. Agricultural and Forest Meteorology 102: 213-222
Pubmed: Author and Title
CrossRef: Author and Title
Google Scholar: Author Only Title Only Author and Title

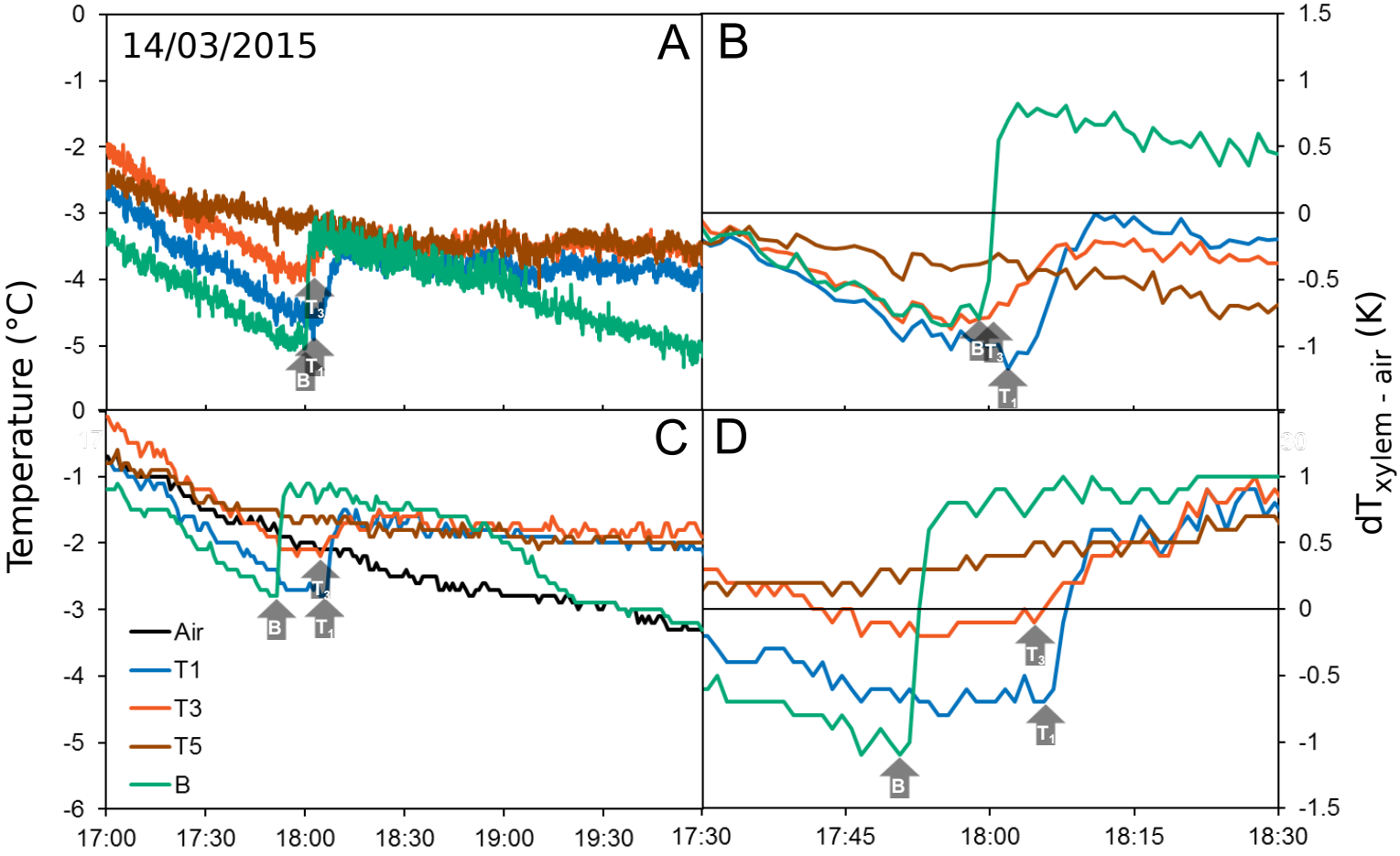

Figure S1. Freezing patterns monitored via infrared imaging (A, B) and thermocouples (C, D) . Left panels (A, C) show absolute temperatures, right panels (B, D) show differential thermal analysis (xylem - air temperature) during the same freezing event. Arrows indicate the onset of exotherms at different sensor positions (B, T_1, T_3), according to Fig. 1.